

Speciation and Attenuation of Arsenic and Selenium at Coal Combustion By-Product Management Facilities

Volume 2: Arsenic

Final Report
October 1, 2002 - September 30, 2005

Mr. Robert Patton

U.S. Department of Energy
National Energy Technology Laboratory
626 Cochrans Mill Road
PO Box 10940, MS 922-273C
Pittsburgh, PA 15236-0940

DOE Award Number: DE-FC26-02NT41590

Principal Investigators:

L. Lee, Purdue University
I. Murarka, Ish Inc.

Submitted By:

K. Ladwig
Electric Power Research Institute
3412 Hillview Avenue
Palo Alto, CA 94304

EPRI DISCLAIMER OF WARRANTIES AND LIMITATION OF LIABILITIES

THIS DOCUMENT WAS PREPARED BY THE ORGANIZATION(S) NAMED BELOW AS AN ACCOUNT OF WORK SPONSORED OR COSPONSORED BY THE ELECTRIC POWER RESEARCH INSTITUTE, INC. (EPRI). NEITHER EPRI, ANY MEMBER OF EPRI, ANY COSPONSOR, THE ORGANIZATION(S) BELOW, NOR ANY PERSON ACTING ON BEHALF OF ANY OF THEM:

(A) MAKES ANY WARRANTY OR REPRESENTATION WHATSOEVER, EXPRESS OR IMPLIED, (I) WITH RESPECT TO THE USE OF ANY INFORMATION, APPARATUS, METHOD, PROCESS, OR SIMILAR ITEM DISCLOSED IN THIS DOCUMENT, INCLUDING MERCHANTABILITY AND FITNESS FOR A PARTICULAR PURPOSE, OR (II) THAT SUCH USE DOES NOT INFRINGE ON OR INTERFERE WITH PRIVATELY OWNED RIGHTS, INCLUDING ANY PARTY'S INTELLECTUAL PROPERTY, OR (III) THAT THIS DOCUMENT IS SUITABLE TO ANY PARTICULAR USER'S CIRCUMSTANCE; OR

(B) ASSUMES RESPONSIBILITY FOR ANY DAMAGES OR OTHER LIABILITY WHATSOEVER (INCLUDING ANY CONSEQUENTIAL DAMAGES, EVEN IF EPRI OR ANY EPRI REPRESENTATIVE HAS BEEN ADVISED OF THE POSSIBILITY OF SUCH DAMAGES) RESULTING FROM YOUR SELECTION OR USE OF THIS DOCUMENT OR ANY INFORMATION, APPARATUS, METHOD, PROCESS, OR SIMILAR ITEM DISCLOSED IN THIS DOCUMENT.

DOE DISCLAIMER

THIS REPORT WAS PREPARED AS AN ACCOUNT OF WORK SPONSORED BY AN AGENCY OF THE UNITED STATES GOVERNMENT. NEITHER THE UNITED STATES GOVERNMENT, NOR ANY AGENCY THEREOF, NOR ANY OF THEIR EMPLOYEES, MAKES ANY WARRANTY, EXPRESS OR IMPLIED, OR ASSUMES ANY LEGAL LIABILITY OR RESPONSIBILITY FOR THE ACCURACY, COMPLETENESS, OR USEFULNESS OF ANY INFORMATION, APPARATUS, PRODUCT, OR PROCESS DISCLOSED OR REPRESENTS THAT ITS USE WOULD NOT INFRINGE PRIVATELY OWNED RIGHTS. REFERENCE HEREIN TO ANY SPECIFIC COMMERCIAL PRODUCT, PROCESS, OR SERVICE BY TRADE NAME, TRADEMARK, MANUFACTURER, OR OTHERWISE DOES NOT NECESSARILY CONSTITUTE OR IMPLY ITS ENDORSEMENT, RECOMMENDATION, OR FAVORING BY THE UNITED STATES GOVERNMENT OR ANY AGENCY THEREOF. THE VIEWS AND OPINIONS OF AUTHORS EXPRESSED HERIN DO NOT NECESSARILY STATE OR REFLECT THOSE OF THE UNITED STATES GOVERNMENT OR ANY AGENCY THEREOF.

ABSTRACT

This report contains results of the laboratory batch equilibrium studies for chemical attenuation of arsenic species by soils from three coal-fired power plant sites. Several soil samples were collected from three power plant sites to conduct the laboratory chemical attenuation studies. Adsorption isotherms and coefficients were developed for both arsenic(III) and arsenic(V) species. Physical and chemical characterization data for the soils were obtained so that correlations between soil properties and adsorption of arsenic species can be established to the extent possible. Linear, Freundlich, and Langmuir adsorption isotherms were fitted to the data as appropriate.

The effects of calcium and sulfate, the dominant ionic constituents in coal ash leachates, on the adsorption of the As(III) and As(V) by soils were measured. The effects of pH on arsenic species adsorption by soils were also measured. Sequential leaching studies were performed on coal ash samples collected from each of the three landfill sites. Kinetic leaching tests on ash samples were also performed.

Adsorption of arsenic species was generally non-linear with respect to concentration. For all three sites, adsorption of As(V) was significantly greater than As(III). Linear distribution coefficients calculated from adsorption isotherms at a concentration of 1 mg/L ranged from about 30 to 350 L/kg for As(V), and from about 5 to 50 L/kg for As(III). The impact of sulfate concentrations on adsorption were soil dependent and most pronounced for As(III). In general sulfate tends to decrease adsorption of arsenic species onto the soils. Adsorption of As(V) was generally enhanced by calcium in solution but As(III) adsorption was not much influenced by calcium.

Linear regression analysis of the adsorption coefficients and soil chemical and physical properties indicates that the best correlation was found with 15-second DC extractable iron. However, reasonably good correlations were also found for percent clay content and for DC-extractable Fe and Al in soils.

These chemical attenuation data for the arsenic species can be used to model arsenic migration in groundwater at the coal ash management sites for the coal fired power plant sites.

CONTENTS

1 INTRODUCTION	1-1
Objectives	1-1
Literature Review	1-1
2 METHODS AND MATERIALS	2-1
Soil Sampling and Characterization	2-1
Adsorption Isotherms on Site Soils	2-2
Data Analysis	2-3
Matrix Effects Studies.....	2-5
pH Effect on Arsenic Adsorption	2-6
Fly Ash Leaching.....	2-6
Moisture Content	2-6
Sequential Leaching.....	2-6
Kinetic Leaching	2-7
Attenuation by Soils of Arsenic in Leachate	2-7
3 ARSENIC ADSORPTION ON SITE SOILS.....	3-1
NE Site	3-1
Soil Characterization Data.....	3-1
Arsenic Adsorption on NE Site Soils	3-1
SE Site	3-6
Soil Characterization Data.....	3-6
Arsenic Adsorption on SE Site Soils.....	3-7
MW Site.....	3-12
Soil Characterization Data.....	3-12
Arsenic Adsorption on MW Site Soils	3-13
4 FACTORS AFFECTING ARSENIC SORPTION	4-1
Solution pH Effect on Arsenic Adsorption	4-1

Solution Matrix Effects on Arsenic Adsorption	4-6
Sorption Data versus Soil Characteristics for All Sites.....	4-11
5 ATTENUATION OF ARSENIC IN ASH LEACHATE	5-1
Sequential Leaching.....	5-1
Leaching Kinetics	5-1
Leachate Arsenic Attenuation by NE Site Soils.....	5-2
6 REFERENCES	6-1

LIST OF FIGURES

Figure 2-1 Sorption by a NE site soil sample from a single solution concentration of As(V) measured at several times, and a complete multi-concentration sorption isotherm measured after 48 hours. C_s =sorbed concentration; C_w =solution concentration.....	2-3
Figure 3-1 As(V) sorption isotherms for NE site soils.	3-3
Figure 3-2 As(III) sorption isotherms for NE site soils.....	3-4
Figure 3-3 As(V) and As(III) sorption for NE site soils using NE1 25-30 soil (solid line) and NE2 10-15 soil (dashed line). Upper plots are isotherms; lower plots show concentration-specific K_d^*	3-6
Figure 3-4 As(V) sorption isotherms for SE site soils.	3-9
Figure 3-5 As(III) sorption isotherms for SE site soils.....	3-10
Figure 3-6 As(V) and As(III) sorption for SE site soils using SE2 33.5-35.5 soil (solid line) and SE3 60-75 soil (dashed line). Upper plots are isotherms; lower plots show concentration-specific K_d^*	3-12
Figure 3-7 As(V) sorption isotherms on MW site soils.	3-15
Figure 3-8 As(III) sorption isotherms on MW site soils.	3-16
Figure 3-9 As(V) and As(III) sorption for MW site using MW3 23-25 soil (solid line) and MW1 17-19 soil (dashed line). Upper plots are isotherms; lower plots show concentration-specific K_d^*	3-18
Figure 4-1 pH effects on As(V) adsorption on NE2 10-15: (a) Arsenate adsorption envelope at varying soil suspension pH values; (b) Arsenate adsorption isotherms at pH 4.0, 4.8, and 5.8.....	4-2
Figure 4-2 pH effects on As(V) adsorption on NE1 25-30: (a) Arsenate adsorption envelope at varying soil suspension pH values; (b) Arsenate adsorption isotherms at pH 4.3, 5.3, and 6.3.....	4-3
Figure 4-3 pH effects on As(III) adsorption on NE2 10-15: (a) Arsenite adsorption envelope at varying soil suspension pH values; (b) Arsenite adsorption isotherms at pH 3.8, 4.8, and 5.8.....	4-4
Figure 4-4 pH effects on As(III) adsorption on NE1 25-30: (a) Arsenite adsorption envelope at varying soil suspension pH values; (b) Arsenite adsorption isotherms at pH 4.8, 5.8, and 6.8.....	4-5
Figure 4-5 Ionic matrix effects on As(V) sorption onto NE2 10-15: (a) Arsenate adsorption envelopes in the presence of varying concentrations of Ca or SO_4 at a constant ionic strength of 0.03M; (b) Arsenate adsorption isotherms in 0.001M $CaCl_2$, 0.001M K_2SO_4 , and 0.001M $CaSO_4$	4-7
Figure 4-6 Ionic matrix effects on As(V) sorption onto NE1 25-30: (a) Arsenate adsorption envelopes in the presence of varying concentrations of Ca or SO_4 at a	

constant ionic strength of 0.03 M; (b) Arsenate adsorption isotherms in 0.001 M CaCl ₂ , 0.001 M K ₂ SO ₄ , and 0.001 M CaSO ₄	4-8
Figure 4-7 Ionic matrix effects on As(III) sorption onto NE2 10-15: (a) Arsenite adsorption envelopes in the presence of varying concentrations of Ca or SO ₄ at a constant ionic strength of 0.03 M; (b) Arsenite adsorption isotherms in 0.001 M CaCl ₂ , 0.001 M K ₂ SO ₄ , and 0.001 M CaSO ₄	4-9
Figure 4-8 Ionic matrix effects on As(III) sorption onto NE1 25-30: (a) Arsenite adsorption envelopes in the presence of varying concentrations of Ca or SO ₄ at a constant ionic strength of 0.03 M; (b) Arsenite adsorption isotherms in 0.001 M CaCl ₂ , 0.001 M K ₂ SO ₄ , and 0.001 M CaSO ₄	4-10
Figure 4-9 Correlation for As(V) (upper graph) and As(III) (lower graph) between Freundlich K _f values and easily reducible Fe assayed using a 15-second DCB extraction.....	4-13
Figure 5-1 pH profile over sequential leaching series for ash samples collected from 15-20 ft depth in two cores at the NE site.	5-2
Figure 5-2 As(III) and As(V) profiles over sequential leaching series for ash samples collected from 15-20 ft depth in two cores at the NE site.	5-3
Figure 5-3 Batch leaching of As(III) and As(V) from NE ash samples versus time up to a maximum 30-day equilibration period.	5-3
Figure 5-4 Attenuation of As(III) (upper plot) and As(V) (lower plot) present in ash leachate by two NE site soils, and multi-concentration arsenic isotherms measured from 0.001 M CaSO ₄	5-4

LIST OF TABLES

Table 3-1 Selected properties of 6 soils representative of the NE site.	3-2
Table 3-2 Isotherm fits for arsenate [As(V)] adsorption from 0.001 M CaSO ₄ for NE site soils.	3-5
Table 3-3 Isotherm fits for arsenite [As(III)] adsorption from 0.001 M CaSO ₄ for NE site soils.	3-5
Table 3-4 Selected properties of 6 soils representative of the SE site.	3-8
Table 3-5 Isotherm fits for As(V) adsorption from 0.001 M CaSO ₄ for SE site soils.	3-11
Table 3-6 Isotherm fits for As(III) adsorption from 0.001 M CaSO ₄ for SE site soils.	3-11
Table 3-7 Selected properties of 6 soils representative of the MW site.	3-14
Table 3-8 Isotherm fits for As(V) adsorption from 0.001 M CaSO ₄ for MW site soils.	3-17
Table 3-9 Isotherm fits for As(III) adsorption from 0.001 M CaSO ₄ for MW site soils.	3-17
Table 4-1 Summary of linear regressions between various soil parameters and the mass-based Freundlich isotherm sorption coefficients.	4-11
Table 4-2 Summary of linear regressions between various soil parameters and the Langmuir model fits for C _{s, max} (mg/kg).	4-12
Table 4-3 Summary of linear regressions between various soil parameters and the Langmuir model fits for mass-based Langmuir K _L values.	4-12

1

INTRODUCTION

Chemical attenuation of arsenic in subsurface soils is highly dependent on the arsenic species present in solution (leachate) and the characteristics of the soil. This project was designed to evaluate chemical attenuation of As(III) and As(V) at three coal-fired power plant sites. One site is located in the northeastern United States (NE), one site is located in the Southeast (SE), and one site is located in the Midwest (MW). These data can be used to model arsenic migration in groundwater at the sites for comparison to monitoring well data. This report presents the results of laboratory determinations of attenuation characteristics for soils collected from the three sites.

Objectives

The overall objectives of this research project were to:

- Collect soil samples from each of the three power plant sites and characterize them for selected physical and chemical properties,
- Conduct laboratory batch equilibrium experiments to develop adsorption isotherms and coefficients for both As(III) and As(V) species from multiple soil samples from each of the three sites,
- Collect coal ash samples from the three power plants and perform sequential batch leaching tests to characterize arsenic release from these ashes, and
- Carry out laboratory batch tests to assess the effects of ash leachate composition and pH on the chemical attenuation of both As(III) and As(V) species by the three site soils.

Literature Review

The widespread occurrence of arsenic in soils and groundwater from both natural and anthropogenic sources has spawned considerable public and regulatory interest pertaining to the environmental impact of arsenic in drinking water. The toxicity and mobility of arsenic species in the subsurface environment are dependent on its reduction-oxidation (redox) state. Under chemically oxidizing conditions, the As(V) species predominates and exists as oxyanions of arsenic acid (H_2AsO_4^- between pH 2.2-7.0 and HAsO_4^{2-} above pH 7). Under chemically reducing conditions, the As(III) species is dominant and exists as arsenious acid (H_3AsO_3^0) below a pH of 9.2. The As(III) species is considerably more toxic than As(V), and is usually reported to be more weakly bound to most mineral surfaces compared to As(V) (Goldberg 2002; Goldberg & Johnston 2000; Manning & Goldberg 1997).

A large body of research is currently available on the adsorption of arsenic on both pure mineral surfaces and soil particles (EPRI, 2000). Inorganic constituents of soils that have been recognized to adsorb significant amounts of arsenic include Fe and Al oxides/oxyhydroxides (hereafter referred to as Fe and Al oxides), alumino-silicates, and carbonates. Both As(V) and As(III) have strong affinities to adsorb onto Fe and Al oxides; however, the two species behave differently with regard to the influence of pH. In the pH range of 3 to 9, adsorption of As(V) onto both Fe and Al oxides is reported to be at the maximum and decreases with increasing pH (Goldberg 2002; Manning & Goldberg 1996; Xu et al., 1988; Pierce & Moore 1982; Anderson et al., 1976), while As(III) adsorption generally increases with increasing pH up to a maximum at pH 7 to 8 (Goldberg 2002; Manning & Goldberg 1997; Pierce & Moore 1982; Gupta & Chen 1978). Adsorption of arsenic species onto alumino-silicate clay minerals (kaolinite, illite, and montmorillonite) may also be appreciable, but to a far lesser degree than adsorption onto Fe and Al oxides. Arsenate [As(V)] adsorption onto kaolinite, illite, and montmorillonite is highest at low pH values, exhibiting an adsorption maxima in the pH 3 to 7 range, and decreases at higher pH (Goldberg 2002; Manning & Goldberg 1996; Goldberg & Glaubig 1988). Arsenite [As(III)] adsorption on each of these alumino-silicates minerals increases up to a pH of 9 (Goldberg 2002; Manning & Goldberg 1997). Under alkaline environments adsorption of arsenic onto carbonate minerals may also be substantial. Capacities for arsenic adsorption onto calcite fall between those reported for Fe and Al oxides and clay minerals, with both As(V) and As(III) adsorption increasing with increasing pH up to a maximum at around pH 10 (Goldberg & Glaubig 1988; Brannon & Patrick 1987).

Aside from pH, Eh, and soil mineral composition, the ionic composition of the interstitial water of soils also impacts arsenic adsorption. Anionic constituents such as phosphate and sulfate may directly compete with either arsenic species for available surface binding sites, or indirectly influence arsenic adsorption by altering the electrostatic charge at solid surfaces (Jain & Loeppert 2000). Adsorption of As(V) onto Fe oxides, gibbsite, and alumino-silicates is significantly reduced in the presence of phosphate (Jain & Loeppert 2000; Manning & Goldberg 1996a). However, the competitive effects of sulfate anions on As(V) adsorption are dependent on the sorbent. Adsorption of As(V) onto amorphous Fe oxides is only slightly affected by sulfate (Jain & Loeppert 2000; Wilkie & Hering 1996), while As(V) adsorption onto alumina is significantly decreased in the presence of sulfate, although to a much lesser extent than would be caused by phosphate anions (Xu et al., 1988). As(III) adsorption by Fe oxides is significantly decreased by both phosphate and sulfate with phosphate having a greater effect (Jain & Loeppert 2000; Wilkie & Hering 1996). Some types of sorption sites appear to have a higher selectivity for As(III) than either sulfate or phosphate (Jain & Loeppert 2000).

Calcium has been shown to enhance the adsorption of both As(V) and As(III) by soils with As(III) generally being less enhanced than As(V) (Smith et al., 2002). Although the detailed mechanisms of this enhancement have not been well documented, the specific adsorption of cations onto soil surfaces likely plays a significant role in mediating the charge on the adsorbing surfaces. Specifically adsorbed cations can shift the charge potential in the plane of sorption to be more negative, thereby increasing anion sorption (Smith et al., 2002; Bowden et al., 1973 & 1977; Bolan et al., 1993). An alternative mechanism may be the formation of intra-molecular bridges between As(V) ions and negatively charged surface sites (e.g., organic matter and alumino-silicate surfaces) by the divalent cations.

Published literature also suggests a potentially significant microbial role in altering the redox state of arsenic such that the dominant redox state in the field may be contrary to predictions based on chemical parameters alone. Microbial populations do both reduce and oxidize arsenic depending on whether they are trying to detoxify arsenic or using it to shuttle electrons during metabolic activity.

One of the anthropogenic sources of arsenic to the environment is leachate derived from coal ash disposal facilities. During the combustion of coal in the utility boilers, arsenic contained in organic matter and sulfide compounds in coal is volatilized into combustion gases (Eary et al.,1990). Once these gases, and fly ash particles entrained in the gases, are vented from the combustion furnace they quickly cool down leading to the condensation of relatively soluble oxides or inorganic salts of arsenic onto the surface of fly ash particles (Eary et al.,1990; Theis et al.,1982; Theis & Wirth 1977).

The enrichment of arsenic on the surfaces of fly ash particles substantially increases its potential for leaching giving rise to elevated concentrations in leachates. EPRI (1987) reported ranges between < 0.1 and 0.51 mg/L in water soluble arsenic in hot-water extracts (1:20 mass-to-volume ratio at 105°C) of 38 fly ash samples from various source coals and combustion technologies. Jackson and Miller (1998) reported a similar range between < 0.001 and 1.65 mg/L As in (1:40 mass-to-volume ratio at room temperature) water extracts of 23 fly ash samples. Additionally, Jackson and Miller (1998) reported that As(V) was the primary redox species found in nearly all of the water extracts, with As(III) typically below the limits of detection. In contrast, varying amounts of As(III) were measured by Turner (1981) in aqueous extracts of 12 fly ash samples, with As(III) comprising between 2% and 66% of soluble arsenic.

Adsorption onto soil surfaces is a dominant chemical attenuation mechanism for arsenic in leachate released from unlined coal ash disposal facilities. In order to establish a theoretical framework to predict arsenic species attenuation by soil contacted by ash leachate, this study focused on the following objectives: (1) characterizing the adsorption of As(V) and As(III) onto power plant site soils having a wide range of physical and chemical properties; (2) establishing a range of partition coefficients that may be used in assessing the retardation of arsenic in ash leachate by soils; (3) quantifying the competitive effects of Ca and SO₄ on the adsorption of As(V) and As(III); (4) quantifying pH effects on arsenic species adsorption; and (5) if possible, developing a predictive tool for estimating arsenic species attenuation by soil using easily quantifiable soil and solution properties.

2

METHODS AND MATERIALS

Soil Sampling and Characterization

Soils samples were collected from several depths at each of the three sites by split spoon sampling equipment with a plastic insert. Two to three soil borings were advanced within about 200 feet of the downgradient edge of the ash fill using a hollow stem auger, and samples were collected at five to ten foot intervals. The samples were sealed in the field in two foot sections with end caps and then taped so that the plastic tubes endured the shipping without spilling out the samples. Several soil samples were collected from each of the soil borings and if appropriate were composited in the laboratory from consecutive depths. The soil samples were shipped to the laboratory in chilled coolers. Ash samples from the landfill site were collected in a similar manner. Soil samples were also collected underneath the ash landfill at the northeastern power plant site. The other two sites could not be samples underneath the ash landfill due to engineering considerations.

Upon arrival at the laboratory at Purdue University, soil and ash samples were transferred to plastic bins, and stored moist (or dry if moisture was not present in the samples) at 4°C. Soil pH and texture was used to screen samples received in order to select a subset of samples considered representative of the site for use in the adsorption studies. For each sample selected, a subsample (≈ 200 g) was air dried, sieved to particle diameter less than 2 mm, and thoroughly homogenized prior to chemical/physical characterization and use. Each processed soil sample was characterized for the following physical and chemical properties: particle size distribution by the hydrometer method (Grossman & Reinsch, 2002), pH of 1:1 (5 g soil: 5 mL H₂O) soil suspensions, pH of 1:1 (5 g soil:5 mL CaCl₂) soil suspensions, cation exchange capacity (Chapman, 1965), dithionite-citrate extractable iron and aluminum (Loeppert & Inskeep, 1996), acid ammonium oxalate extractable iron and aluminum (Loeppert & Inskeep, 1996), percent base saturation (by summation of 1M NH₄⁻ extractable basic cations), percent organic matter (Nelson & Sommers, 1996), Bray P1 extractable phosphorus (Bray and Kurtz 1945), X-ray diffraction analysis of clay minerals, and timed dithionite-citrate-bicarbonate (DCB) extractions of Fe and Al.

The dominant clay minerals in each of the soil samples were measured using an x-ray diffraction analysis method. Briefly, 15 g of soil was homogenized and sieved at 2 mm followed by carbonate removal (soil reacted with 50-mL 1 M ammonium acetate, pH = 5) and removal of organics and manganese oxides via soil digestion with 30-mL 30% H₂O₂ at 45°C. The soil was then dispersed by sonication, and the clay size fraction of particles fractionated by a centrifugation scheme intended to separate particles at 2 μ m. The clay size fraction was then frozen using liquid nitrogen and freeze-dried for later analysis. For each soil, two slides were

prepared for x-ray diffraction. These slides consisted of samples which either had been K-saturated or had been Mg-saturated and glycerol solvated. X-ray diffraction patterns of the clay size fraction were obtained using $\text{CuK}\alpha$ radiation and a type F Siemens Diffractometer with omega drive. The diffractometer was equipped with a 1 degree divergence slit, 0.25° receiving slit, 0.4° scatter slit, and a graphite monochromator. Samples were scanned from 2 to $30^\circ 2(\theta)$ using a 0.02 degree increment and a 1 second count time. During the analysis the K-saturated samples were analyzed after being exposed to four separate temperature regimes (room temperature, 100°C , 300°C , and 550°C).

Timed dithionite-citrate-bicarbonate (DCB) extractions of soils were performed by accurately weighing 2 g of sodium dithionite into a 250-mL beaker containing 50-mL 0.3 M sodium citrate and 0.2 M sodium bicarbonate. A shaft-driven stirrer was placed into the solution and the stir rate was adjusted to 200 rpm. One gram of soil was then quickly added to the DCB solution. A small aliquot (~ 2 mL) of this suspension was then drawn from the beaker after 15 seconds using a 10 mL plastic syringe. The aliquot drawn from the beaker was quickly filtered by passing it through a $0.45\ \mu\text{m}$ regenerated cellulose syringe filter. Filtered samples were analyzed for iron and aluminum using flame atomic adsorption spectrophotometry (FAAS).

Adsorption Isotherms on Site Soils

Adsorption isotherms were constructed independently for both As(V) and As(III) in an ionic matrix of 10^{-3} M CaSO_4 using a minimum of four As concentrations and up to eight concentrations plus zero As control. Applied solution concentrations generally ranged from 0.2 to 5 mg/L in the case of As(V), and 0.3 to 1.2 mg/L for As(III). Arsenic solutions were added to 50 mL polypropylene centrifuge tubes containing 0.5 g to 1 g (oven dried weight, o.d.w) of soil to obtain solid suspension densities of 20 g/L for As(V) and 50 g/L for As(III). Soil suspensions were then allowed to equilibrate at $22 \pm 2^\circ\text{C}$ on a rotary shaker (~ 45 RPM) for 48 h for As(V) and 16 h for As(III). Arsenic concentrations in solution were measured after equilibration (C_w , mg/L), and sorbed concentrations (C_s , mg/kg) were estimated by the difference in the As mass applied and the As mass remaining in solution after equilibration with soil.

Equilibration times were selected to achieve near equilibrium without having significant shifts in the redox state of the As remaining in solution; the redox state of sorbed As was assumed to be the same as what was measured in the initial solution. In the preliminary kinetic experiments, total As was determined by atomic adsorption/graphite furnace (GFAA), As(III) by AA/HVG, and As(V) by difference between total As and As(III) concentrations, which was confirmed with inductively coupled plasma-mass spectrometry (ICP-MS). Suspensions containing As(III) were equilibrated for a shorter period of time due to concerns that a significant amount of As(III) would oxidize to As(V) within a 48 hour equilibration period. Based on preliminary work (Figure 2-1), and previous studies by Pierce and Moore (1982), who found that 99% of adsorption on soils takes place within 9 hours, the equilibration time in each case was sufficient to attain near equilibrium conditions.

After equilibration, the pH of the soil suspensions was measured using an Accumet® AR25 pH meter in conjunction with an Accumet® double junction glass pH electrode. Ten milliliters of suspension was collected from each sample and filtered at $0.45\ \mu\text{m}$ using a 10 mL plastic syringe

with a 0.45 μm regenerated cellulose luer-lock syringe filter. Filtered samples were preserved by adding 0.1 mL of concentrated HNO_3 . Analysis of arsenic concentrations in the filtered samples was performed using GFAA.

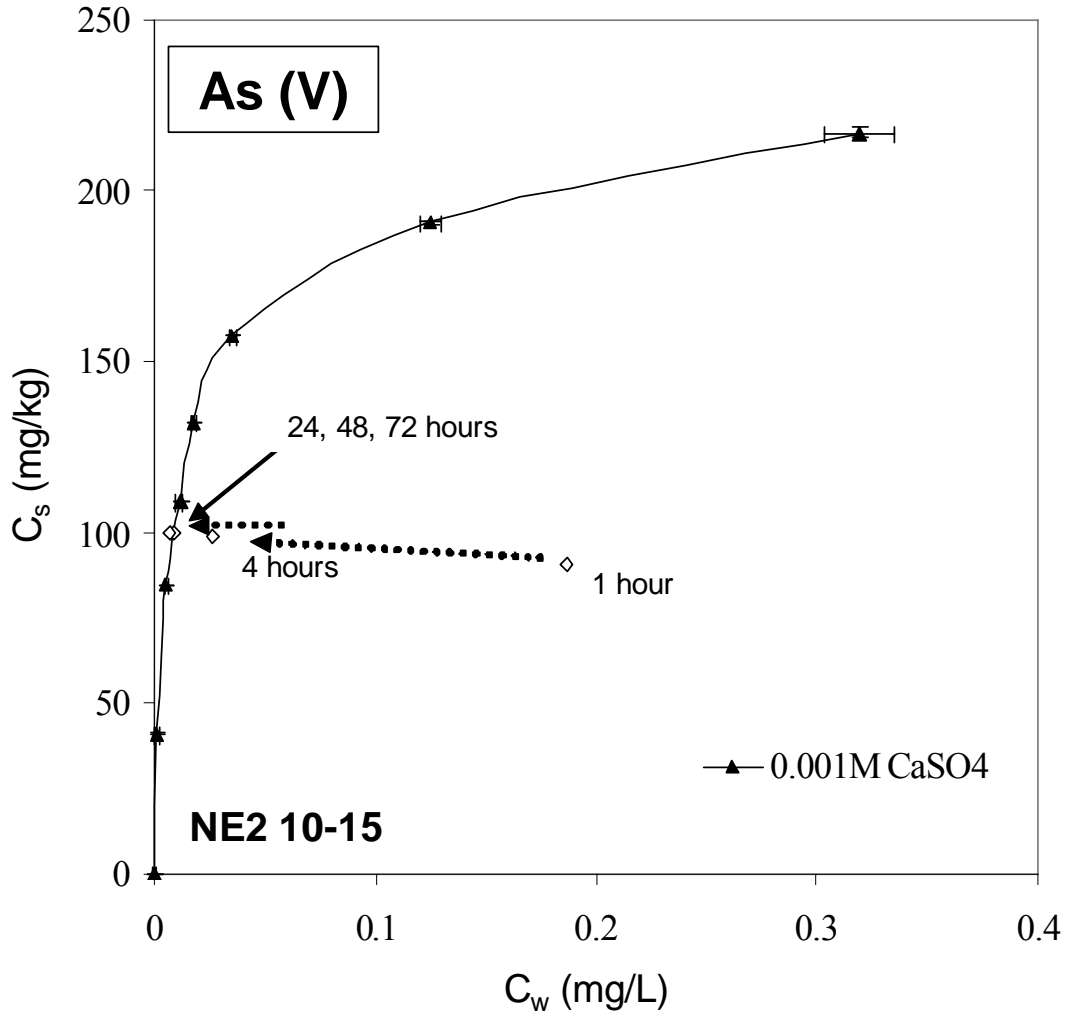


Figure 2-1
Sorption by a NE site soil sample from a single solution concentration of As(V) measured at several times, and a complete multi-concentration sorption isotherm measured after 48 hours. C_s =sorbed concentration; C_w =solution concentration.

Data Analysis

Arsenic isotherms were constructed by plotting sorbed (C_s , mg/kg) versus solution (C_w , mg/L) concentrations and fit using Statistical Analysis System (SAS) v. 8.2 to the three sorption models most commonly used to describe the sorption behavior of a chemical over a specified concentration range.

$$C_s = K_d C_w \quad \text{Linear} \quad (2-1)$$

$$C_s = K_f C_w^N \quad \text{Freundlich} \quad (2-2)$$

$$C_s = \frac{K_L C_{s,\max} C_w}{1 + K_L C_w} \quad \text{Langmuir} \quad (2-3)$$

where C_s (mg/kg) is the chemical concentration in the soil at equilibrium; C_w (mg/L) is the chemical concentration in the aqueous phase at equilibrium; K_d (L/kg) is the linear sorption coefficient; K_f is the Freundlich sorption coefficient, which has units of $\text{mg}^{1-N} \text{L}^N \text{kg}^{-1}$ or $\text{mmol}^{1-N} \text{L}^N \text{kg}^{-1}$ depending on whether you choose to use chemical mass or mole units, and the Freundlich N (unitless), which is a measure of isotherm nonlinearity in the Freundlich equation; K_L (L/mg or L/mmol) is Langmuir affinity coefficient; and $C_{s,\max}$ is the maximum monolayer adsorption capacity (mg/kg). Note that $C_{s,\max}$ reflects the maximum sorption capacity suggesting that all sorption sites are filled assuming site-specific sorption. However, this assumption also does not account for any precipitation that may occur. The regression analysis performed provided best-fit estimates for the parameters of the models along with an estimate of the goodness-of-fit (R^2). Note that both the Freundlich and Langmuir models have sorption coefficients (K_f and K_L) that contain a concentration unit for the chemical; therefore, the magnitude of these values will be different if calculated on a mass scale (e.g., mg) versus a molar scale (e.g., mmol), unlike the linear sorption coefficient (K_d). Also note that for K_f values the conversion is not straightforward because C_w is raised to a power; the difference between mass-based K_f values and mole-based K_f values is, therefore, MW^{N-1} where MW stands for molecular weight (g/mol).

Both the Freundlich and Langmuir models are capable of characterizing the nonlinear sorption behavior of arsenic species. The Freundlich model reflects multi-mechanistic sorption and/or sorption sites that range in their sorption affinities. The Langmuir model was derived assuming that there is a maximum number of sites on the soil surface ($C_{s,\max}$) to which a solute can adsorb. The Freundlich model collapses to the linear sorption model when N is exactly equal to one, and approaches the Langmuir model at small values of N . The $C_{s,\max}$ estimated using Langmuir model fits to isotherms constructed from a limited concentration range can be in error; typically isotherms are not constructed using high enough solute concentrations to achieve the true $C_{s,\max}$. Also, as higher solute concentrations are applied to the soil, the soil surface can be sufficiently changed such that other sorption mechanisms or precipitation chemistry become operational, thus a true $C_{s,\max}$ may not actually be achieved.

The Freundlich model is often the best approach to predicting sorption as a function of concentration when sorption is substantially nonlinear over the concentration range of interest and the specific sorption mechanisms are not known. Problems arise using this approach when predictive transport models only allow for the input of a linear sorption coefficient (K_d). In the latter case, the model can estimate a concentration-specific K_d^* value using the Freundlich isotherm model coefficients (K_f and N):

$$K_d = K_f C_w^{N-1} \quad (2-4)$$

Note that at $C_w = 1 \mu\text{g/mL}$ using a mass-based K_f value, $K_d^* = K_f$ (likewise for $C_w = 1 \mu\text{mol/mL}$ using a mole-based K_f). For isotherms with Freundlich N values less than one, K_d^* increases as C_w values decrease. Therefore, when an incoming solution (e.g., fly ash leachate) first contacts the soil given $N < 1$, the operational K_d is the highest and becomes smaller (thus less attenuation) as the concentration in the pore-water becomes equal to the incoming solution (e.g., $C_w = C_i$). This nonlinear ($N < 1$) behavior results in a solute breakthrough curve (C_w versus pore volumes past through the soil matrix), for example at a well, that exhibits a self sharpening front. Eventually after the incoming solution is void of the chemical, the chemical concentration profile will exhibit an extended tail.

Matrix Effects Studies

The effects of Ca and SO_4 , the dominant ionic constituents of many coal ash leachates, on the adsorption of As(V) and As(III) were characterized on two soils (NE2 10-15 and NE1 25-30) having considerably different capacities to adsorb arsenic. Two types of experiments were conducted for each arsenic species on both soils. In the first set of experiments, adsorption of two different initial concentrations of either As(V) or As(III) was quantified as a function of solution concentrations of Ca or SO_4 for each As concentration. In the second set of experiments, adsorption isotherms of each arsenic species were produced in 10^{-3} M KCl, 10^{-3} M CaCl_2 , 10^{-3} M K_2SO_4 , and 10^{-3} M CaSO_4 at eight initial concentrations of As(V) or As(III).

Arsenic solutions for the adsorption envelope experiments were prepared by poisoning the ionic strength of solutions containing 0, 10^{-4} , $10^{-3.3}$, 10^{-3} , $10^{-2.3}$, and 10^{-2} M CaCl_2 or K_2SO_4 to an ionic strength of 0.03 M using 1M KCl. Small aliquots of 1,000 mg/L As(V) or As(III) (from $\text{Na}_2\text{HAsO}_4 \cdot 7\text{H}_2\text{O}$ or NaAsO_2) were then spiked into the appropriate solution matrix to obtain initial As concentrations of 1 mg/L and 0.75 mg/L, respectively. Arsenic solutions were then added to 50-mL polypropylene centrifuge tubes containing 0.5 grams o.d.w. (oven dried weight) soil in duplicate to obtain solid suspension densities of 10 g/L for As(V) and 25 g/L for As(III). Equilibration and analysis were as previously described for the determination of the multi-concentration isotherms. Arsenic speciation analysis of selected samples, using ion chromatography-inductively coupled plasma-mass spectroscopy (IC-ICP-MS), confirmed that conversion of As(III) to As(V) was insignificant during the 16 h equilibration time at all pH values observed in the experiments.

Arsenic solutions for adsorption isotherm experiments consisted of 10^{-3} M KCl, 10^{-3} M CaCl_2 , 10^{-3} M K_2SO_4 , and 10^{-3} M CaSO_4 . No attempts were made at controlling the ionic strength of the equilibrating solutions; however, the effect of ionic strength on arsenic sorption is reported to be negligible for the range of ionic strengths used in the current study ($10^{-3} - 10^{-2.4}$ M) (Goldberg and Johnston, 2001; Manning and Goldberg, 1997). Adsorption of each arsenic species was measured in duplicate at eight concentrations in the concentration range of 0 to 3 mg/L for As(V) and 0 to 1 mg/L for As(III). All other experimental protocols, including solid suspension

densities, equilibration times, and sampling regimes, were identical to those described for the fixed As concentration experiments.

pH Effect on Arsenic Adsorption

Similar to the matrix effect studies, the effects of pH on arsenic species adsorption were characterized for the same two soils using two types of experiments. In the first set of experiments, adsorption of fixed initial concentrations of either As(V) or As(III) in 10^{-3} M KCl was quantified as a function of solution pH yielding a profile referred to as an adsorption envelope or pH-edge. In the second group of experiments, As(V) and As(III) adsorption isotherms from 10^{-3} M KCl were produced at the native pH of the soil, and at pH values that were one pH unit above and below the native soil pH. The arsenic solution of either 1 mg/L As(V) or 0.5 mg/L As(III) was adjusted to a desired range of pH values (3 to 11) using 0.25 M KOH or HCl. Multi-concentration arsenic adsorption isotherms at the native soil pH \pm 1 pH unit were constructed using six As concentrations in duplicate by varying the initial concentrations of both As(V) or As(III) from 0 to 1 mg/L As. All other experimental protocols, including solid suspension densities, equilibration times, and sampling regimes, were identical to those used in the adsorption envelope studies.

Fly Ash Leaching

Moisture Content

Fly ash samples were stored in an airtight container to ensure no evaporation took place after collection. Moisture contents were determined by weighing the moist ash into a pre-weighed container, placed in an oven at 105°C for 24 hours, cooled to room temperature in a desiccator, and re-weighing. Moisture content was estimated by the difference in moist and oven-dried weights.

Sequential Leaching

Sequential leaching studies were performed in triplicate for ash samples collected at 15-20 feet below ground surface (bgs) in cores NE3 and NE4. Approximately 20 g of ash and 68 g of reagent-grade water (Barnstead Nanopure System) were added to 80-ml Nalgene polycarbonate test tubes. All tubes were rotated end-over-end and allowed to equilibrate for 24 hours, followed by centrifugation at 2,700 RPM for 1 hour using the Jouan Laboratory Equipment Centrifuge, model CR422. Values of pH were measured and recorded. The supernatant was removed using a Becton Dickinson and Company 10-cc Luer Lok syringe, filtered using Alltech 0.45- μ m cellulose filters, and split into two subsamples of which one was acidified with two drops of concentrated (70%) trace-metal grade nitric acid and the other with 2 drops of concentrated HCl. Acidified samples were stored in acid-washed Nalgene polyethylene or polypropylene bottles with polypropylene screw closures. Reagent-grade water was then added to the ash remaining in the tube to replace the solution removed, and the leaching procedure was repeated 10-15 times. Samples were analyzed using the Thermo Jarrell Ash ICP (model AtomScan16) in combination

with a CETAL Technologies Ultrasonic Nebulizer (model U5000AT+) or using the AA/GF furnace as previously described.

Kinetic Leaching

Kinetic leaching studies were performed in duplicate from the same ash samples. Approximately 12.5 g of ash and 43 g of reagent-grade water (Barnstead Nanopure System) were added to acid-washed 60-ml Nalgene polycarbonate test tubes. For each time increment, a set of duplicate tubes were destructively sampled. All tubes were rotated end-over-end and allowed to equilibrate for specified time increments that include: 2 h, 4 h, 8 h, 1 d, 2 d, 4 d, 8 d, 12 d, 20 d, and 30 d. Tubes were centrifuged at 2,000 RPM for 20 minutes using the Jouan Laboratory Equipment Centrifuge (Model CR422). Values of pH and subsequent arsenic concentrations were determined as previously described.

Attenuation by Soils of Arsenic in Leachate

Fly ash leachate obtained from a first sequential leaching of ash from the NE site was spiked with 150 ppb As(V) and 50 ppb As(III) and applied to soils at mass (g) to volume (mL) ratios of 1:100, 1:40, and 1:20. Samples were rotated end-over-end, followed by quantification of As(V) and As(III) in the solution phase of the soil suspensions. Spiked ash leachate was applied at different mass to volume ratio amounts in order to get multiple (C_s , C_w) points without changing the leachate matrix, for a better comparison with multi-concentration isotherms measured from the simulated matrix (0.001 M CaSO_4 in this case).

3

ARSENIC ADSORPTION ON SITE SOILS

NE Site

Soil Characterization Data

Selected soil properties for six soils representative of the NE site are shown in Table 3-1. NE site soils contained 13 to 29% clay composed predominantly of illite and mica with minor amounts of kaolinite. The soils contained less than 1% organic matter and their soil-water pH values ranged from 4.8 to 5.5. Selective Fe dissolution of the soils resulted in DC-extractable Fe (intended to estimate total reducible Fe oxides) levels ranging from approximately 6,000 to 32,000 mg/kg, and DC-extractable Al levels ranging from 270 to 1,300 mg/kg. Ranges in oxalate extractable Fe and Al were less variable, with Fe ranging from 320 to 5,465 mg/kg, and Al ranging from 240 to 513 mg/kg. Based on the assumption that the oxalate extraction primarily dissolves amorphous Fe and Al oxides, the differences between DC and oxalate extracts indicate that 5 to 91% of extractable Fe in the soils is amorphous, and 38 to 89% of extractable Al is amorphous. Fe extracted in 15 seconds with DCB ranged from 270 to 1,618 mg/kg, and was intended to estimate the most reactive portion of Fe oxides (i.e., Fe oxides exposed to solution and readily available for reaction).

Arsenic Adsorption on NE Site Soils

Adsorption data for As(V) and As(III) on the six soils representative of the NE sites were measured and fitted with Freundlich and Langmuir isotherm models. As(V) and As(III) isotherms are plotted in Figures 3-1 and 3-2, and modeling fits are summarized in Tables 3-2 and 3-3. Values of K_f ($\text{mg}^{1-N} \text{m}^N \text{kg}^{-1}$) ranged between 61 and 380 for As(V) sorption, and between 11 and 53 for As(III). Nonlinear sorption is evident for both As(V) (Freundlich N values 0.26 to 0.36 and As(III) (Freundlich N values 0.31 to 0.57). Sorption of As(V) is consistently much higher than that observed for As(III), with Freundlich K_f values being 5 to 9 times higher for As(V); similar trends are evident for the Langmuir $C_{s,\text{max}}$ values as well. To exemplify the overall arsenic sorption behavior by soils at the NE site, As(V) and As(III) isotherms for the lowest and highest sorption observed for the six soil samples were considered representative of the site, as well as the effect of nonlinearity on the concentration-specific K_d^* values that would be used to estimate site-specific transport, are shown in Figure 3-3.

Table 3-1
Selected properties of 6 soils representative of the NE site.

Soil	pH * _{H2O}	pH * _{CaCl2}	Sand %	Silt %	Clay %	CEC (cmol/kg)	DC* - Fe (mg/kg)	DC* - Al (mg/kg)	Ox [†] - Fe (mg/kg)	Ox [†] - Al (mg/kg)	DCB - Fe 15 sec (mg/kg)	Base Saturation %	Organic Matter %	Bray P1- PO ₄ (ppm)	Dominant Clay Minerals
NE1 25-30	5.3	5.1	33	50	17	15.5	5,928	270	320	240	270	87	0.5	38	I, K, V
NE1 35-40	5.0	4.7	40	35	25	12.6	6,030	610	5,465	525	651	62	0.5	2	I, K, V
NE2 10-15	4.8	4.4	60	23	17	4.7	31,800	1,200	1,575	513	992	48	1	10	I, K
NE2 16-21	5.0	4.6	59	28	13	2.45	11,370	630	1,090	364	534	80	0.5	11	I, K
NE3 50-54	5.0	4.9	9	62	29	13.2	22,470	1,070	1,750	475	1,618	64	0.6	14	I, K
NE4 46-50	5.5	5.5	57	28	15	5.8	18,330	1,300	1,590	500	1,044	79	0.9	3	I, K

*dithionite carbonate extractable; † oxalate extractable; I = illite, K = kaolinite, V = vermiculite

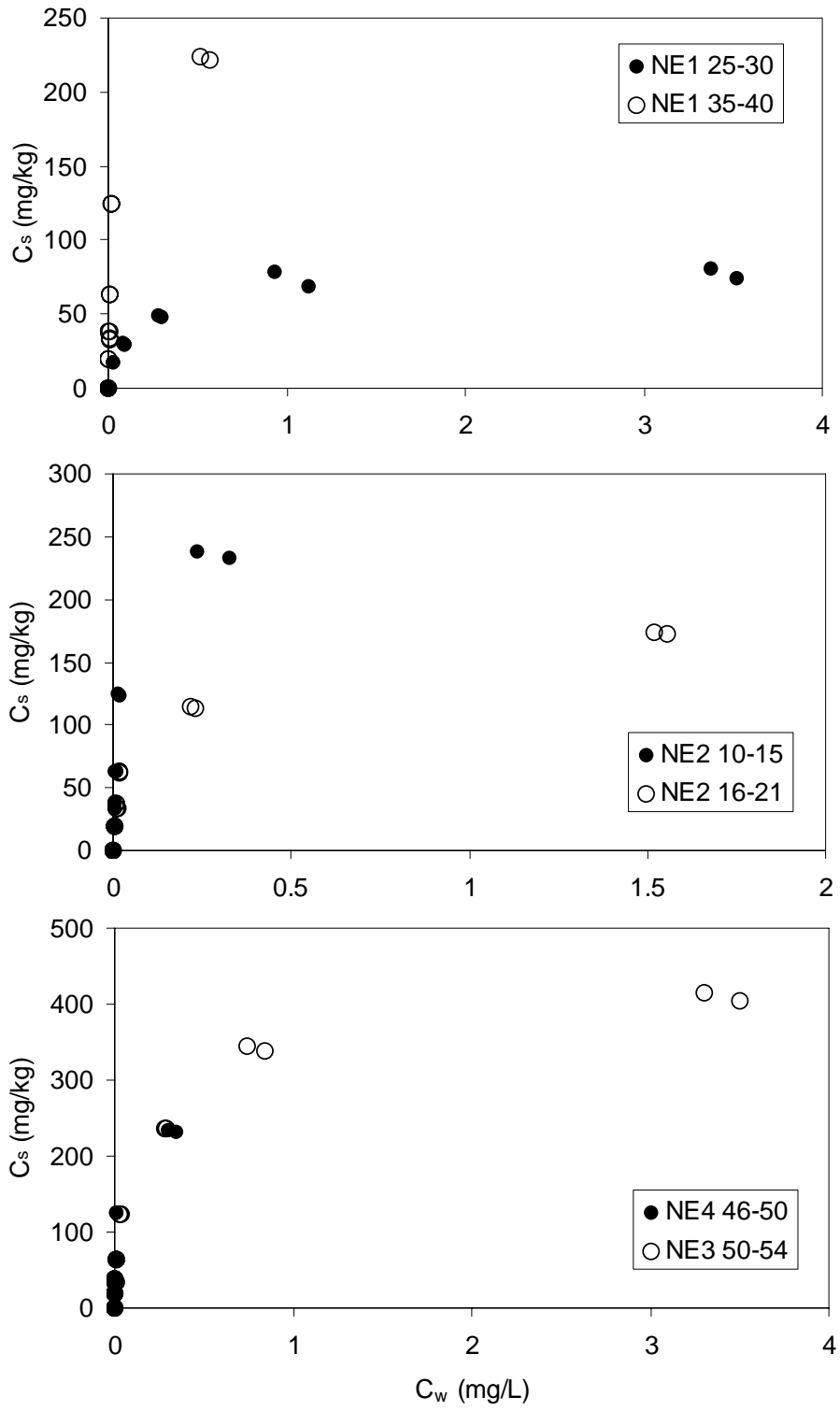


Figure 3-1
As(V) sorption isotherms for NE site soils.

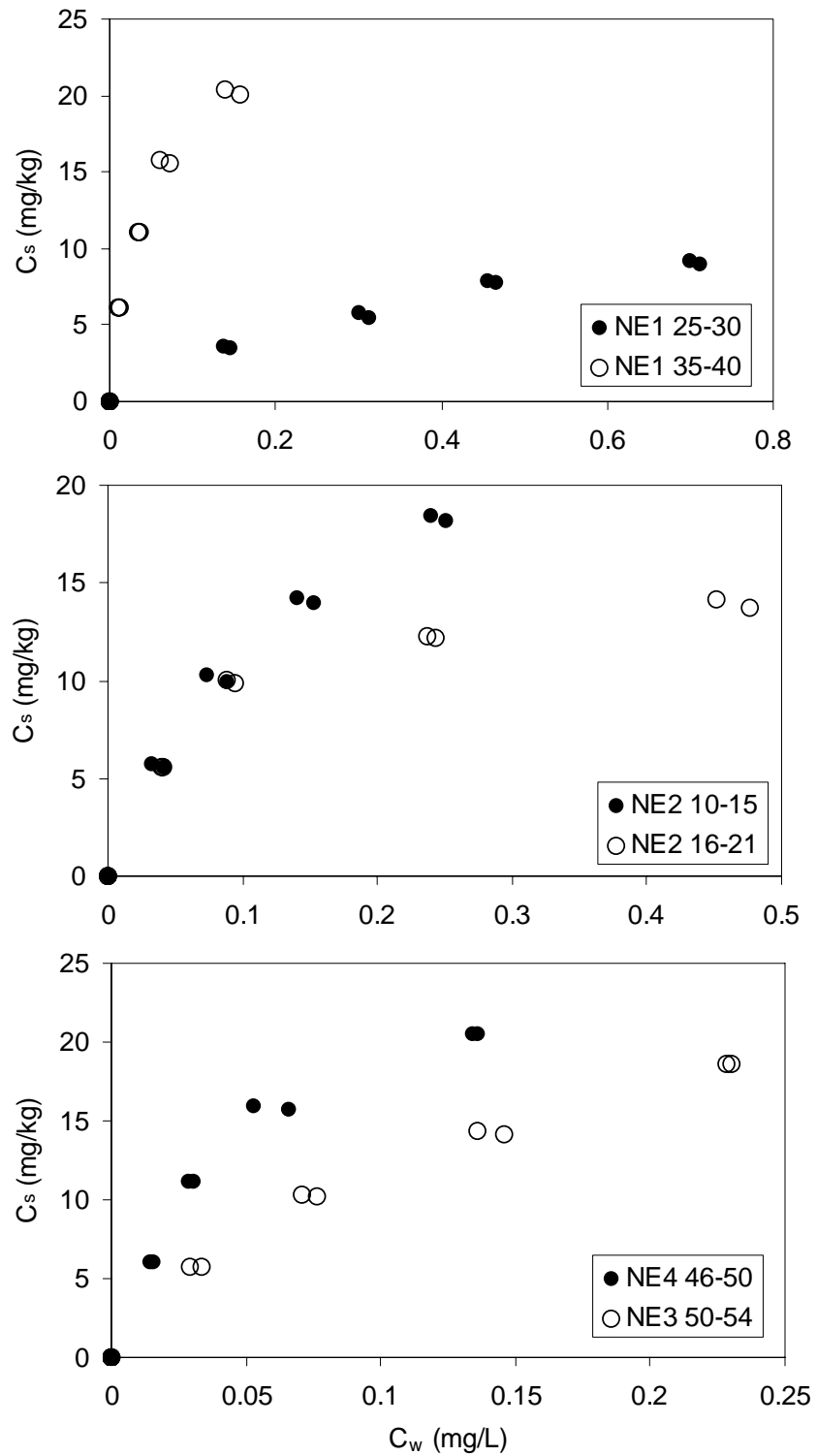


Figure 3-2
As(III) sorption isotherms for NE site soils.

Table 3-2
Isotherm fits for arsenate [As(V)] adsorption from 0.001 M CaSO₄ for NE site soils.

Soil	Freundlich Parameters			Langmuir Parameters		
	K _f	N	r ²	K _L	C _{s,max}	r ²
NE1 25-30	61.3	0.259	0.935	6.6	81.3	0.977
NE1 35-40	275.2	0.31	0.895	47.3	235.2	0.961
NE2 10-15	380.4	0.363	0.93	50	254.9	0.987
NE2 16-21	157.3	0.28	0.975	29	158.8	0.95
NE3 50-54	310.5	0.29	0.968	10.5	387.2	0.967
NE4 46-50	341.1	0.31	0.921	84.1	244.7	0.984

Table 3-3
Isotherm fits for arsenite [As(III)] adsorption from 0.001 M CaSO₄ for NE site soils.

Soil	Freundlich Parameters			Langmuir Parameters		
	K _f	N	r ²	K _L	C _{s,max}	r ²
NE1 25-30	11.4	0.57	0.973	2	15.7	0.982
NE1 35-40	45.7	0.41	0.971	25.5	25.3	0.979
NE2 10-15	41.4	0.57	0.981	6.3	28.9	0.984
NE2 16-21	18.27	0.31	0.91	15.5	15.8	0.977
NE3 50-54	42.8	0.56	0.993	7.3	29.3	0.99
NE4 46-50	53	0.46	0.948	21.8	27.6	0.986

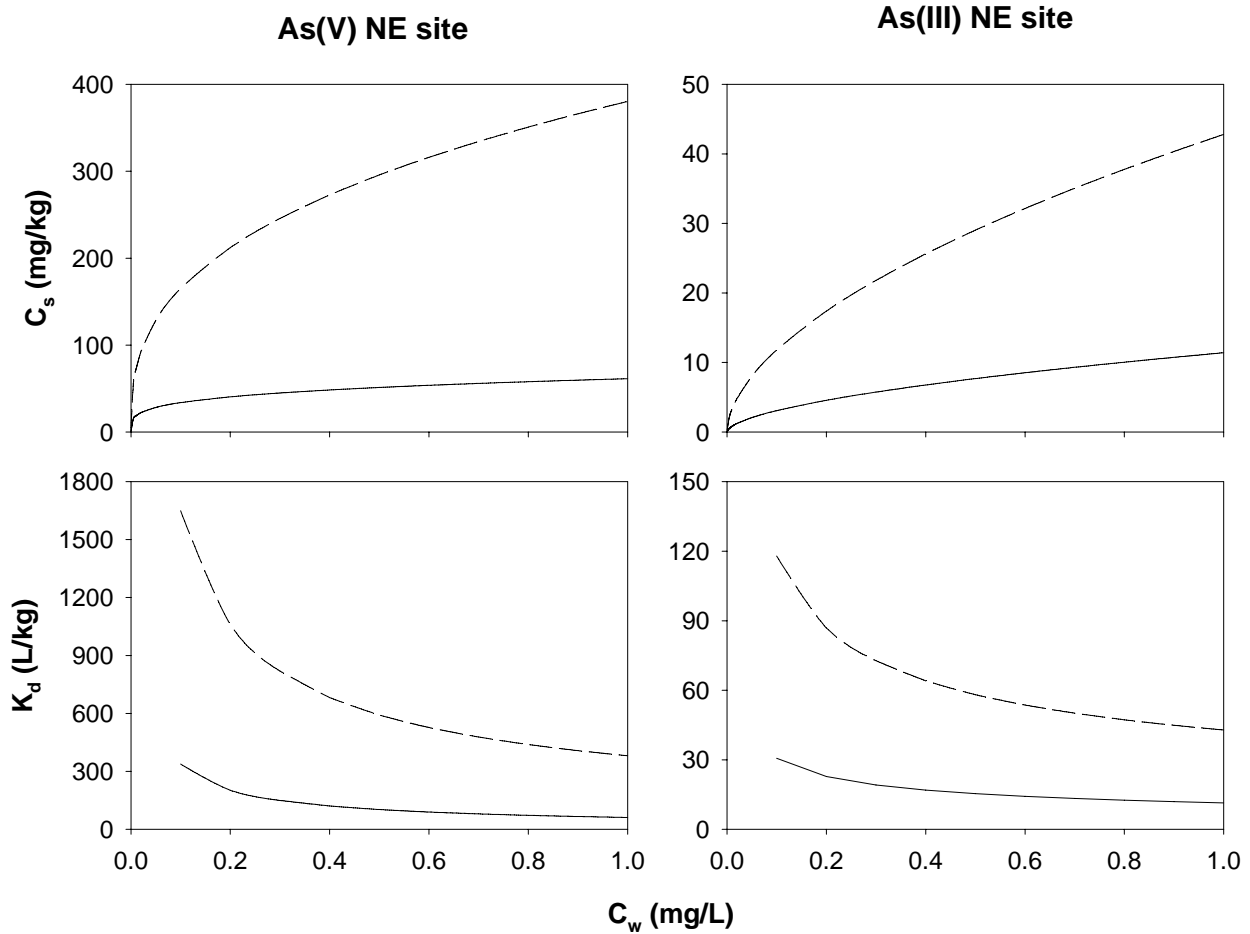


Figure 3-3
As(V) and As(III) sorption for NE site soils using NE1 25-30 soil (solid line) and NE2 10-15 soil (dashed line). Upper plots are isotherms; lower plots show concentration-specific K_d .

SE Site

Soil Characterization Data

Selected soil properties for six soils representative of the SE site are shown in Table 3-4. The SE site soils contained less than 5% clay, which was dominated by kaolinite and illite, with kaolinite being the dominant clay mineral in all soils except SE3 38.5 and SE2 23.5. Soils contained less than 1% organic matter and their soil-water pH values ranged from 5.6 to 6.4. Selective Fe dissolution of the soils resulted in DC-extractable Fe levels ranging from approximately 5,243 to 14,948 mg/kg, and DC-extractable Al levels ranging from 150 to 900 mg/kg. Ranges in oxalate extractable Fe and Al were less variable, with oxalate extractable Fe ranging from 245 to 757 mg/kg, and oxalate extractable Al ranging from 228 to 486 mg/kg. Based on the assumption

that the oxalate extraction primarily dissolves amorphous Fe and Al oxides, the differences between DC and oxalate extracts indicate that 4 to 8% of extractable Fe in the soils is amorphous, and that half to all of extractable Al is amorphous. Fe extracted in 15 seconds with DCB ranged from 56 to 330 mg/kg, and was intended to estimate the most reactive portion of Fe oxides (i.e., Fe oxides exposed to solution and readily available for reaction).

Arsenic Adsorption on SE Site Soils

Adsorption data for As(V) and As(III) on the six soils representative of the SE site were measured and fitted with Freundlich and Langmuir isotherm models. As(V) and As(III) isotherms are plotted in Figures 3-4 and 3-5, and modeling fits are summarized in Tables 3-5 and 3-6. Values of K_f ($\text{mg}^{1-N} \text{L}^N \text{kg}^{-1}$) ranged between 30 and 184 for As(V) sorption, and between 5 and 23 for As(III), which are lower than observed for NE site soils. Sorption was more nonlinear for SE site soils than NE site soils, with Freundlich N values as low as 0.13 and ranging to 0.28 for As(V) and 0.22 to 0.35 for As(III). Sorption of As(V) is again consistently much higher than that observed for As(III), with Freundlich K_f values being 4 to 14 times higher for As(V); similar trends are evident for the Langmuir $C_{s,\text{max}}$ values as well. To exemplify the overall arsenic sorption behavior at the SE site, As(V) and As(III) isotherms for the lowest and the highest sorption measured for the six soils considered representative of the site soils, as well as the effect of nonlinearity on the concentration-specific K_d^* values that would be used to estimate site-specific transport, are shown in Figure 3-6.

Arsenic Adsorption On Site Soils

Table 3-4
Selected properties of 6 soils representative of the SE site.

Soil	pH * _{H2O}	pH * _{CaCl2}	Sand %	Silt %	Clay %	CEC (cmol/kg)	DC ⁻ - Fe (mg/kg)	DC ⁻ - Al (mg/kg)	Ox [†] - Fe (mg/kg)	Ox [†] - Al (mg/kg)	DCB - Fe 15 sec (mg/kg)	Base Saturation %	Organic Matter %	Bray P1- PO ₄ (ppm)	Dominant Clay Minerals
SE1 48.5-50	5.7	5.4	62	33	5	4.3	7,105	450	576	486	150	72	0.6	8	K, I
SE1 60-62	6.0	5.8	56	39	5	4.8	14,948	900	757	423	330	75	0.7	8	K, I
SE2 23.5-25.5	6.1	6.1	66	31	3	4.1	8,399	182	413	305	56	71	0.3	31	K, I
SE2 33.5-35.5	6.4	6.2	60	35	5	2.7	5,243	280	245	228	60	100	0.2	19	K, I
SE3 5.5-7.5	5.6	5.4	66	29	5	3.1	6,209	280	226	395	84	62	0.4	4	K, I
SE3 38.5-40.5	6.2	6.1	62	35	3	4.1	6,647	150	500	243	73	71	0.4	32	K, I

* dithionite carbonate extractable; † oxalate extractable; I = illite, K = kaolinite

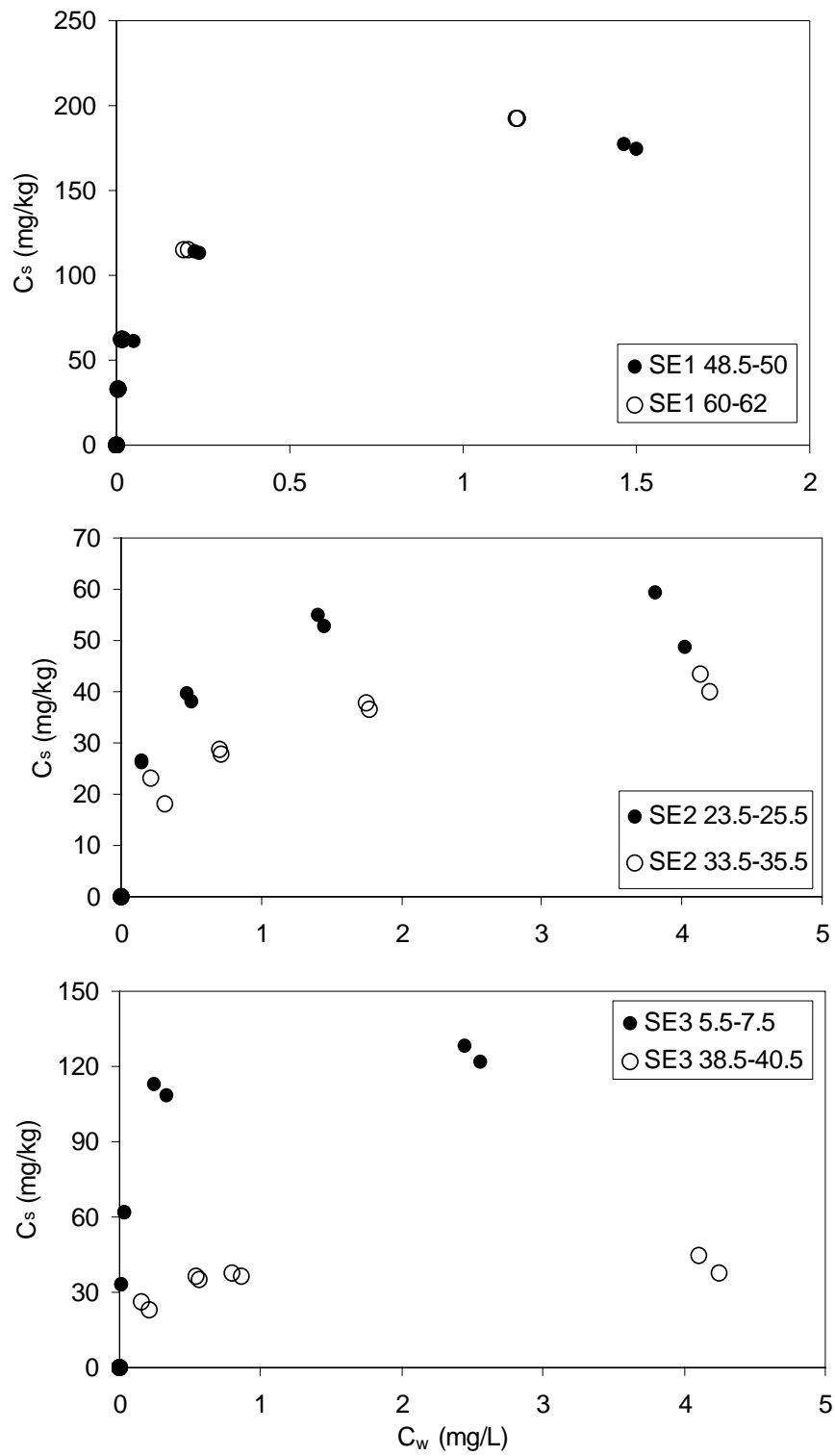


Figure 3-4
As(V) sorption isotherms for SE site soils.

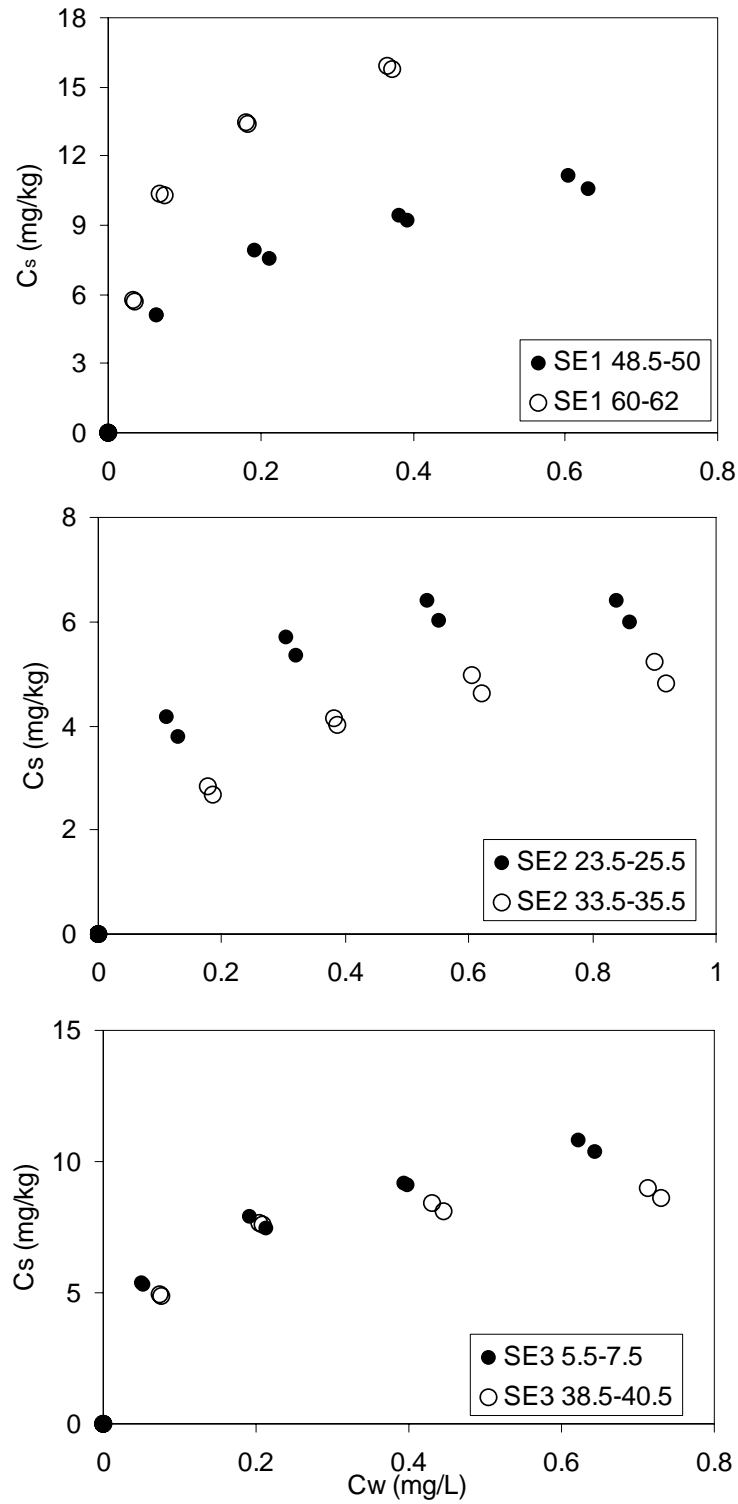


Figure 3-5
As(III) sorption isotherms for SE site soils.

Table 3-5
Isotherm fits for As(V) adsorption from 0.001 M CaSO₄ for SE site soils.

Soil	Freundlich Parameters			Langmuir Parameters		
	K _f	N	r ²	K _L	C _{s,max}	r ²
SE1 48.5-50	160.7	0.28	0.989	12.8	174.9	0.907
SE1 60-62	184.1	0.28	0.997	28.4	173.5	0.909
SE2 23.5-25.5	44.2	0.197	0.879	5.4	57.8	0.943
SE2 33.5-35.5	30.4	0.24	0.941	3	44.2	0.93
SE3 5.5-7.5	113.6	0.174	0.939	40.5	122.9	0.99
SE3 38.5-40.5	35.5	0.132	0.856	8	42.8	0.929

Table 3-6
Isotherm fits for As(III) adsorption from 0.001 M CaSO₄ for SE site soils.

Soil	Freundlich Parameters			Langmuir Parameters		
	K _f	N	r ²	K _L	C _{s,max}	r ²
SE1 48.5-50	12.7	0.32	0.99	10.3	12.1	0.972
SE1 60-62	23.2	0.35	0.975	15.1	18.6	0.994
SE2 23.5-25.5	6.8	0.22	0.837	11.5	7	0.91
SE2 33.5-35.5	5.4	0.35	0.91	4.4	6.4	0.958
SE3 5.5-7.5	11.9	0.272	0.997	15.9	10.9	0.983
SE3 38.5-40.5	9.8	0.22	0.878	14.9	9.7	0.973

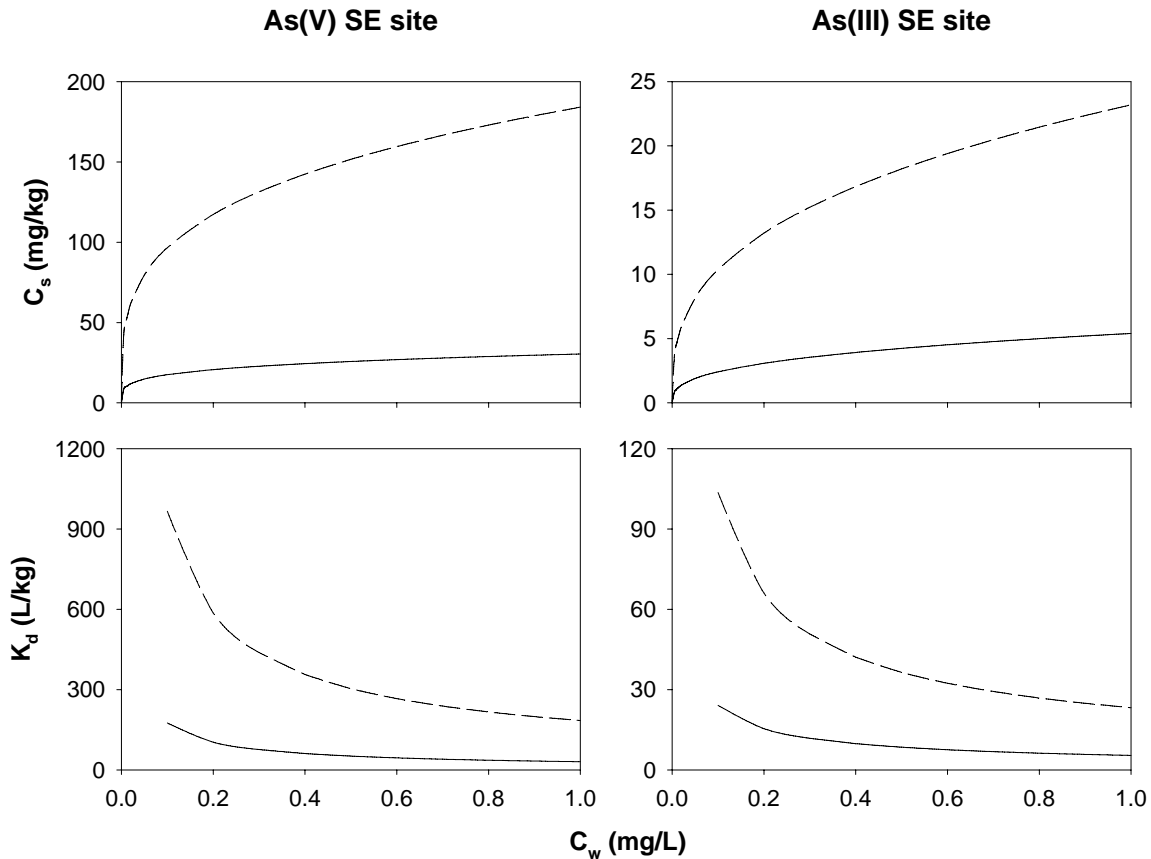


Figure 3-6
As(V) and As(III) sorption for SE site soils using SE2 33.5-35.5 soil (solid line) and SE3 60-75 soil (dashed line). Upper plots are isotherms; lower plots show concentration-specific K_d .

MW Site

Soil Characterization Data

Selected soil properties for six soils representative of the MW site are shown in Table 3-7. Most of the MW site soils contained less than 1% clay; therefore, clay type was not pursued. Soils contained less than 0.5% organic matter and their soil-water pH values ranged from 6.8 to 8.1. Selective Fe dissolution of the soils resulted in DC-extractable Fe levels ranging from 2,718 to 4,540 mg/kg, and DC-extractable Al levels ranging from 175 to 610 mg/kg. Ranges in oxalate extractable Fe and Al were less variable, with oxalate extractable Fe ranging from 217 to 570 mg/kg, and oxalate extractable Al ranging from 78 to 456 mg/kg. Based on the assumption that the oxalate extraction primarily dissolves amorphous Fe and Al oxides, the differences between DC and oxalate extracts indicate that 4 to 13% of extractable Fe in the soils is amorphous, and 39 to 100% of extractable Al is amorphous. Fe extracted in 15 seconds with

DCB ranged from 8 to 69 mg/kg, and was intended to estimate the most reactive portion of Fe oxides (i.e., Fe oxides exposed to solution and readily available for reaction).

Arsenic Adsorption on MW Site Soils

Adsorption data for As(V) and As(III) on the six soils representative of the MW site were measured and fitted with Freundlich and Langmuir isotherm models. As(V) and As(III) isotherms are plotted in Figures 3-7 and 3-8, and modeling fits are summarized in Tables 3-8 and 3-9. Values of K_f ($\text{mg}^{1-N} \text{m}^N \text{kg}^{-1}$) ranged between 28 and 48 for As(V) sorption, and between 5 and 17 for As(III), which are the lowest observed for the soils from the three sites. Although sorption was lowest on the MW site soils, sorption isotherms exhibited less nonlinearity, with Freundlich N values of 0.25 to 0.44 for As(V) and 0.57 to 0.83 for As(III). Sorption of As(V) is consistently higher than that observed for As(III), with both Freundlich K_f values being 2.5 to 7.4 times higher for As(V); similar trends are evident for the Langmuir $C_{s,\text{max}}$ values as well. Differences between As(III) and As(V) were less than observed for the soils at the two other sites. The overall arsenic sorption behavior at the SE site is exemplified in Figure 3-9, with As(V) and As(III) isotherms for the lowest and the highest sorption observed for the six site soils shown, as well as the effect of nonlinearity on the concentration-specific K_d^* values that would be used to estimate site-specific transport.

Table 3-7
Selected properties of 6 soils representative of the MW site.

Soil	pH* _{H2O}	pH* _{CaCl2}	Sand %	Silt %	Clay %	CEC (cmol/kg)	DC* - Fe (mg/kg)	DC* - Al (mg/kg)	Ox [†] - Fe (mg/kg)	Ox [†] - Al (mg/kg)	DCB - Fe 15 sec (mg/kg)	Base Saturation %	Organic Matter %	Bray P1-PO ₄ (ppm)
MW1 17-19	8.1	7.3	93	4	3	3	4540	610	570	456	69	100	0.3	22
MW1 33-35	7.7	6.9	95	4	1	1.4	3781	198	145	78	15	100	0.3	5
MW2 17-19	7.5	6.2	95	4	1	1.4	3312	382	261	253	28	100	0.4	11
MW2 25-27	6.8	6.3	97	2	1	1.4	3143	175	217	95	12	97	0.4	4
MW3 17-19	7.7	6.8	95	4	1	1.7	2718	389	299	384	23	100	0.2	15
MW3 23-25	8.0	6.8	95	4	1	1.4	2964	105	241	105	8	100	0.5	4

* dithionite carbonate extractable; † oxalate extractable

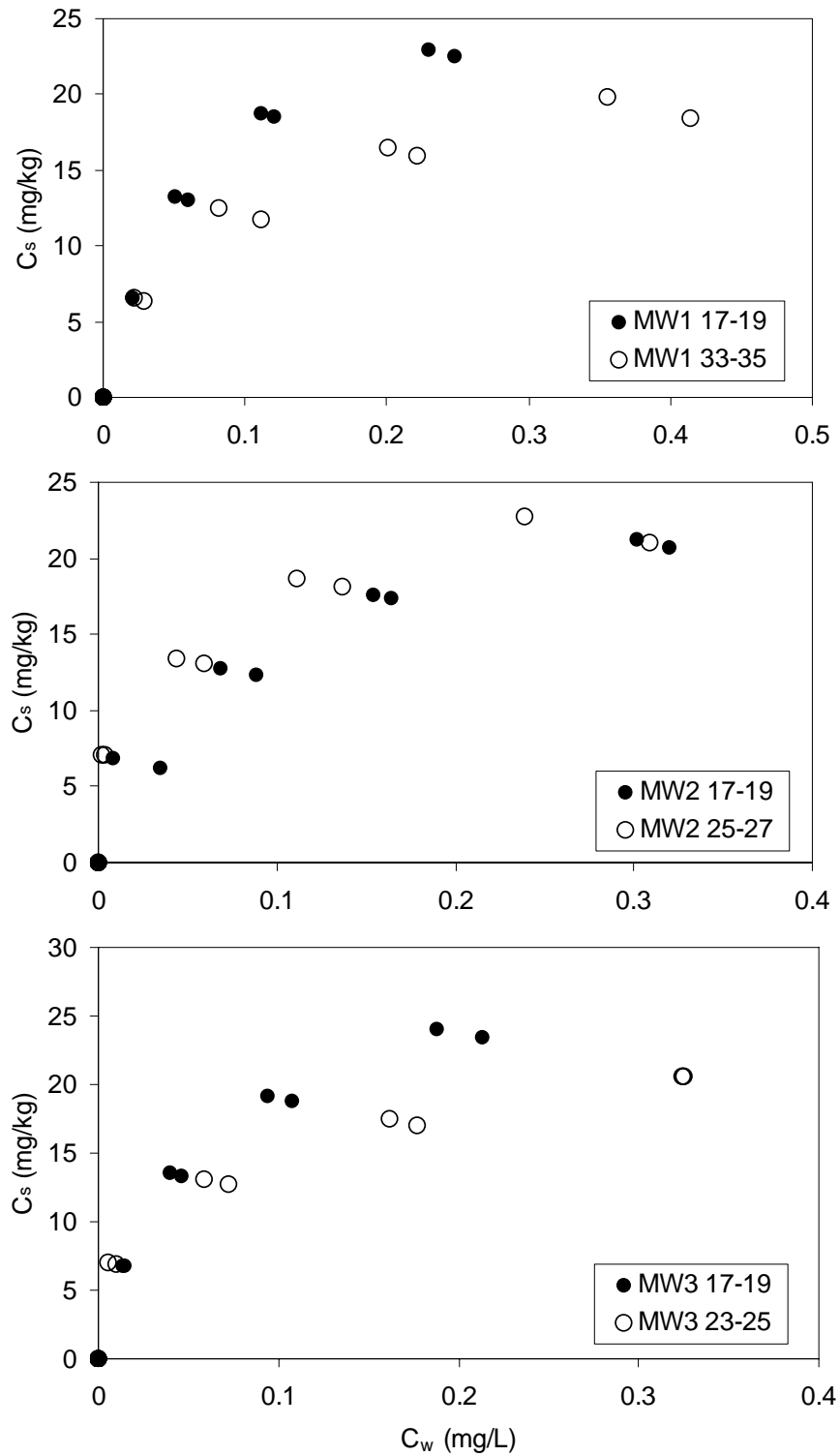


Figure 3-7
As(V) sorption isotherms on MW site soils.

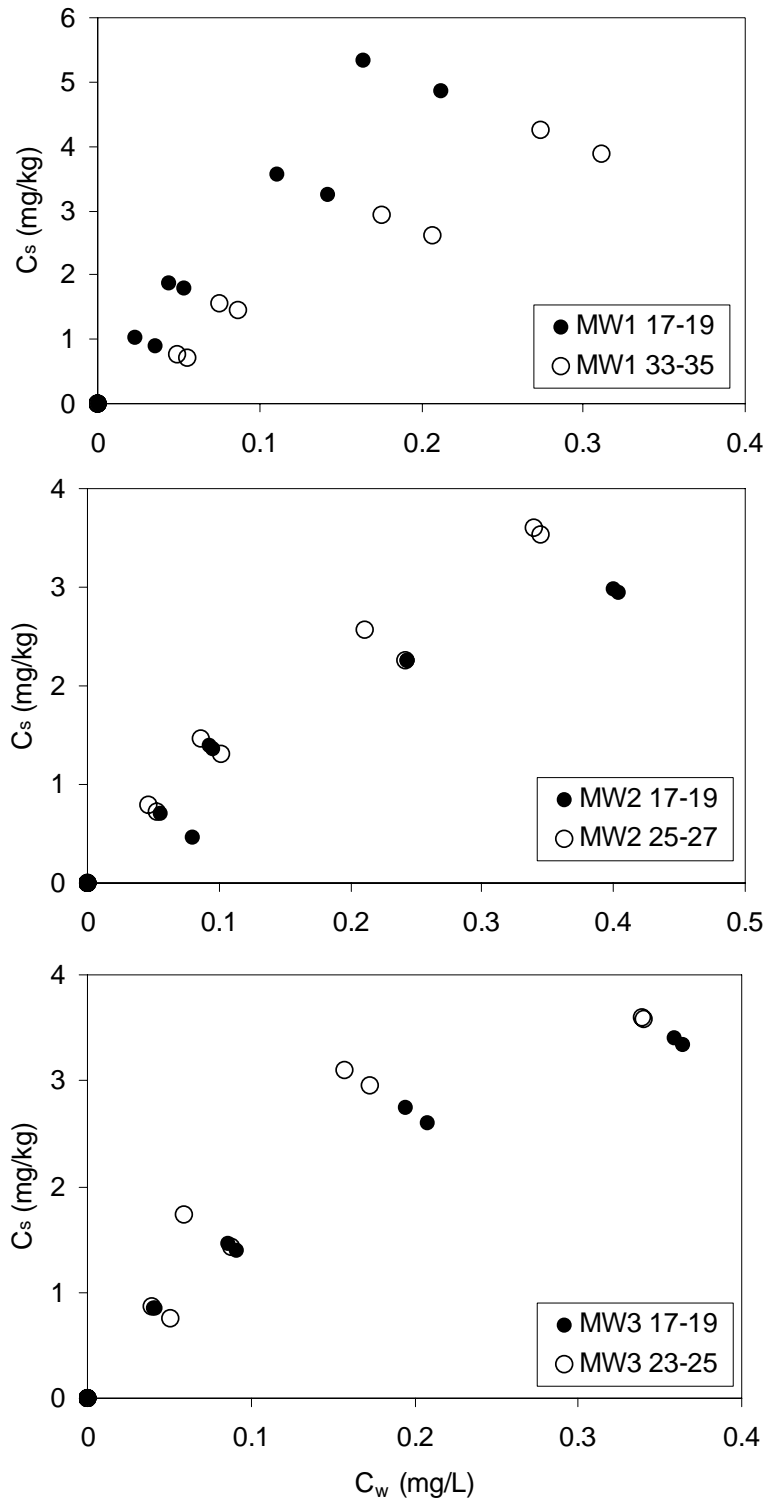


Figure 3-8
As(III) sorption isotherms on MW site soils.

Table 3-8
Isotherm fits for As(V) adsorption from 0.001 M CaSO₄ for MW site soils.

Soil	Freundlich Parameters			Langmuir Parameters		
	K _f	N	r ²	K _L	C _{s,max}	r ²
MW1 17-19	44	0.435	0.967	14.7	29.4	0.996
MW1 33-35	27.6	0.364	0.967	14.5	21.9	0.966
MW2 17-19	33.6	0.387	0.95	12.5	26.1	0.918
MW2 25-27	30.1	0.251	0.967	145.9	19.4	0.825
MW3 17-19	47.6	0.417	0.977	20.2	29.1	0.992
MW3 23-25	28.5	0.29	0.993	40.1	20.5	0.907

Table 3-9
Isotherm fits for As(III) adsorption from 0.001 M CaSO₄ for MW site soils.

Soil	Freundlich Parameters			Langmuir Parameters		
	K _f	N	r ²	K _L	C _{s,max}	r ²
MW1 17-19	16.9	0.747	0.91	3.4	12.3	0.917
MW1 33-35	11.1	0.832	0.949	1.3	14	0.952
MW2 17-19	5.6	0.68	0.938	2	6.8	0.944
MW2 25-27	7.9	0.765	0.972	1.8	8.7	0.966
MW3 17-19	6.4	0.599	0.98	4.1	5.7	0.992
MW3 23-25	7	0.566	0.895	5.2	5.8	0.928

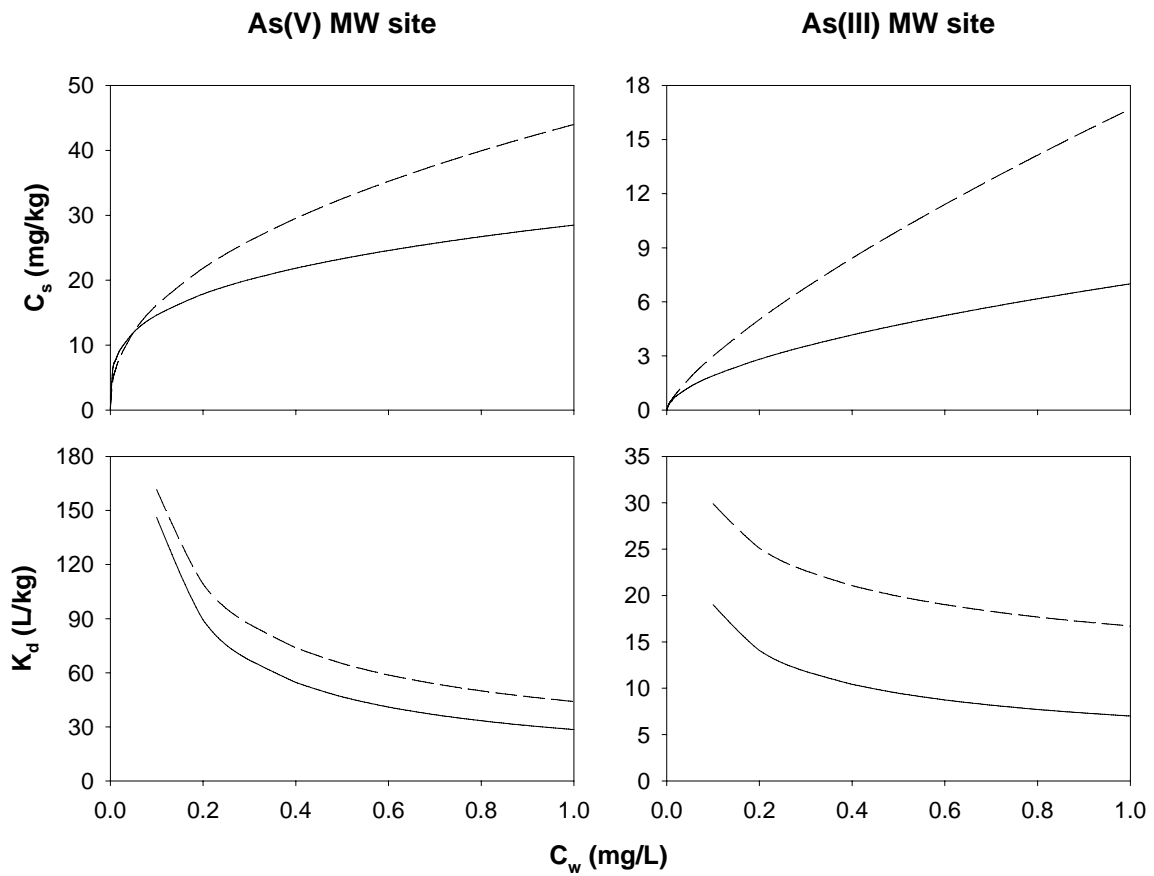


Figure 3-9
As(V) and As(III) sorption for MW site using MW3 23-25 soil (solid line) and MW1 17-19 soil (dashed line). Upper plots are isotherms; lower plots show concentration-specific K_d .

4

FACTORS AFFECTING ARSENIC SORPTION

Solution pH Effect on Arsenic Adsorption

Adsorption envelopes (upper graphs) and adsorption isotherms (lower graphs) produced for each arsenic species, at varying pH values, are shown in Figures 4-1 through 4-4 for two NE site soils. A significant influence of pH on both As(V) and As(III) adsorption is apparent, especially at the more alkaline pH values. However, the influence is small, within ± 1 pH unit of the native soil pH for the NE site soils, which are acidic soils. One exception is As(III) sorption on soil sample NE1 25-30 (Figure 4-4b).

Features of the adsorption envelopes are similar to those reported for pure minerals. For example, As(III) adsorption onto soil sample NE1 25-30 displays an adsorption maxima at a pH greater than 8 (Figure 4-4b), corresponding to the adsorption behavior of As(III) onto aluminum hydroxides or alumino-silicates. For soil sample NE2 10-15, As(III) adsorption corresponded more closely to the reported adsorption behavior of As(III) onto iron oxides, with adsorption remaining relatively constant except at very high or very low pH values (Figure 4-3a). In contrast to As(III), the adsorption envelopes for As(V) for both NE site soils were similar, and corresponded to the behavior reported for arsenate adsorption on iron oxides/oxyhydroxides. As predicted from the pH envelopes and the native soil pH values, the effect of pH near the site-soil pH values on arsenic sorption was negligible except for As(III) sorption by soil sample NE1 25-30.

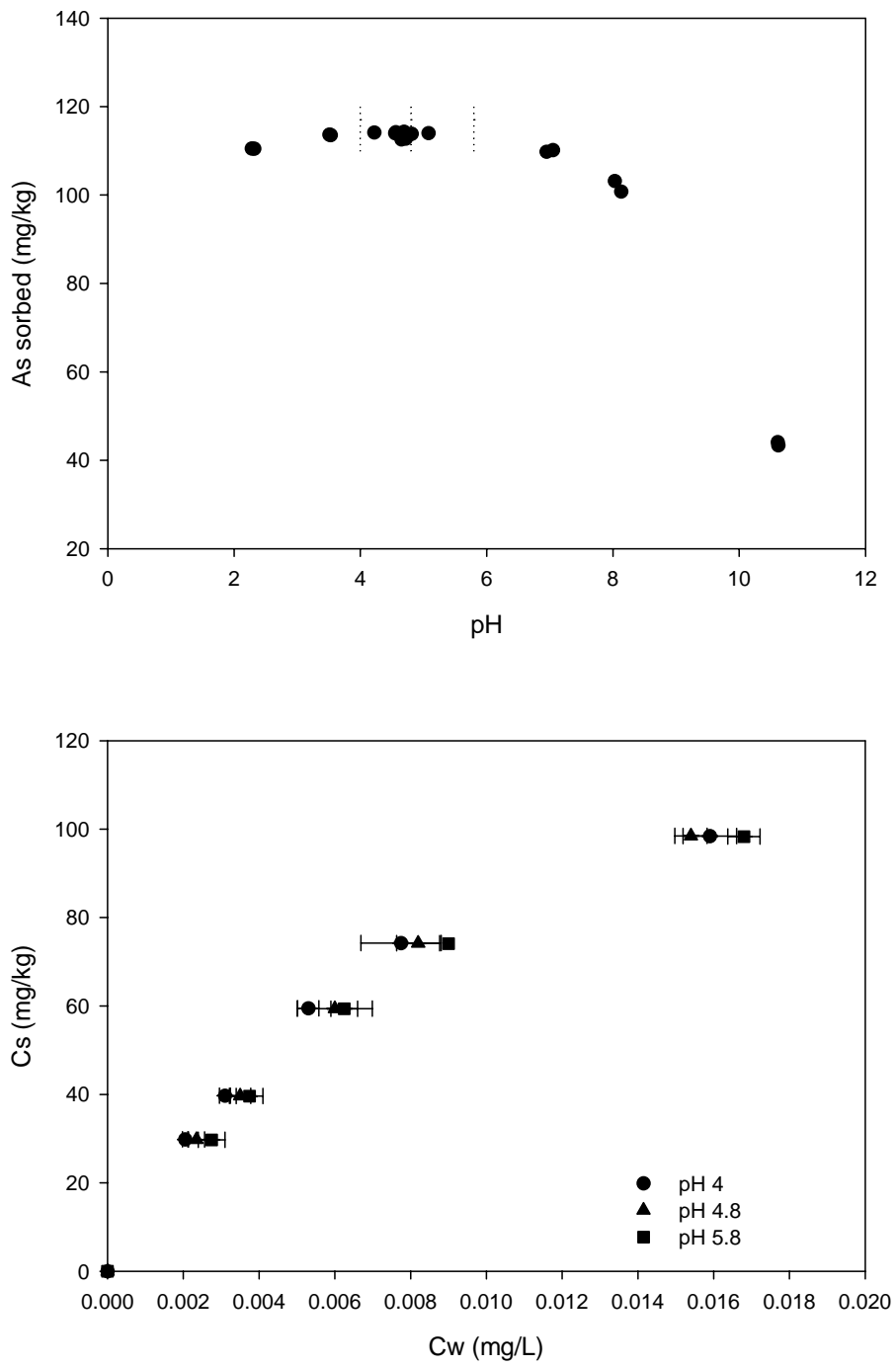


Figure 4-1
pH effects on As(V) adsorption on NE2 10-15: (a) Arsenate adsorption envelope at varying soil suspension pH values; (b) Arsenate adsorption isotherms at pH 4.0, 4.8, and 5.8.

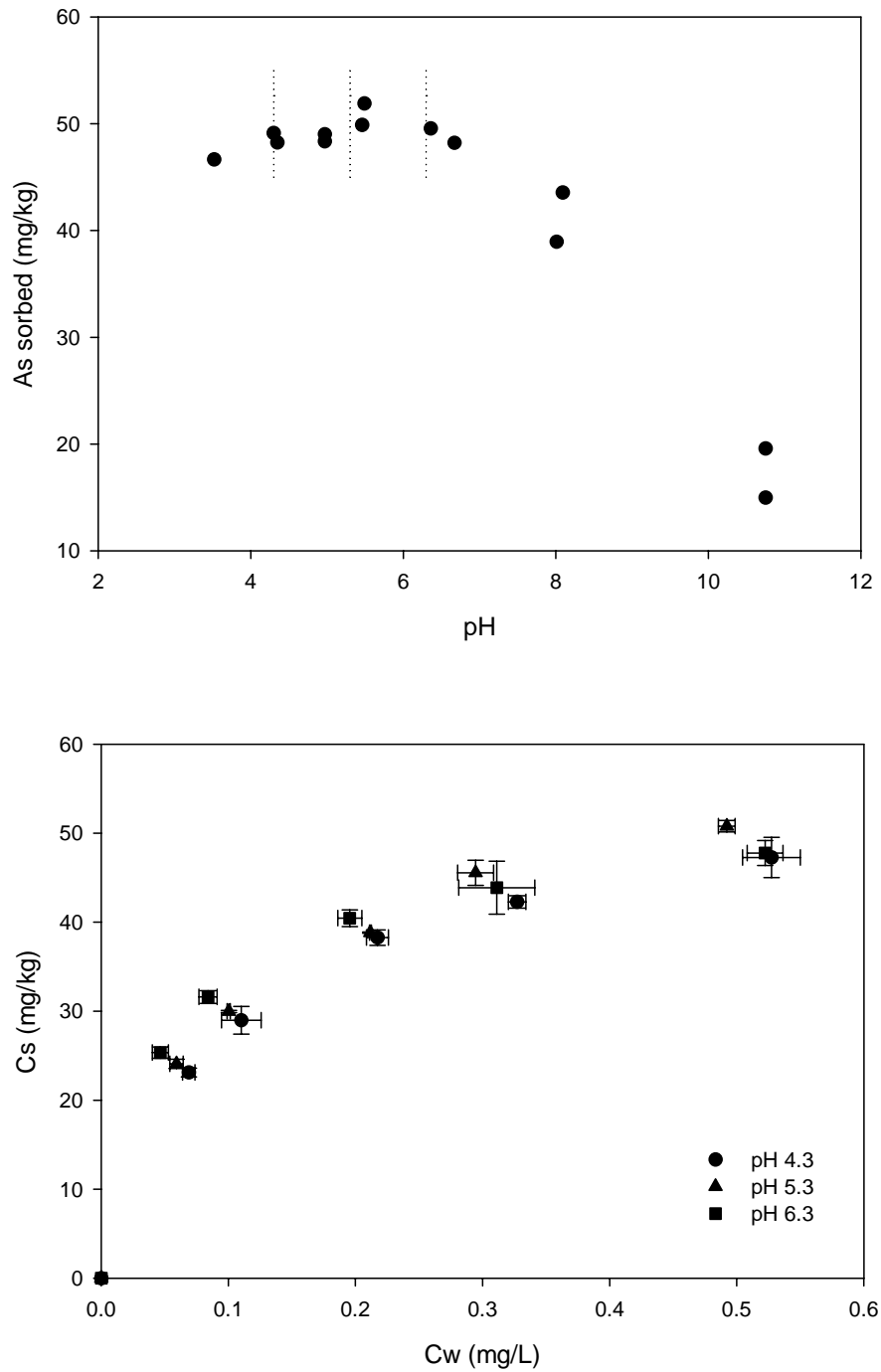


Figure 4-2
 pH effects on As(V) adsorption on NE1 25-30: (a) Arsenate adsorption envelope at varying soil suspension pH values; (b) Arsenate adsorption isotherms at pH 4.3, 5.3, and 6.3.

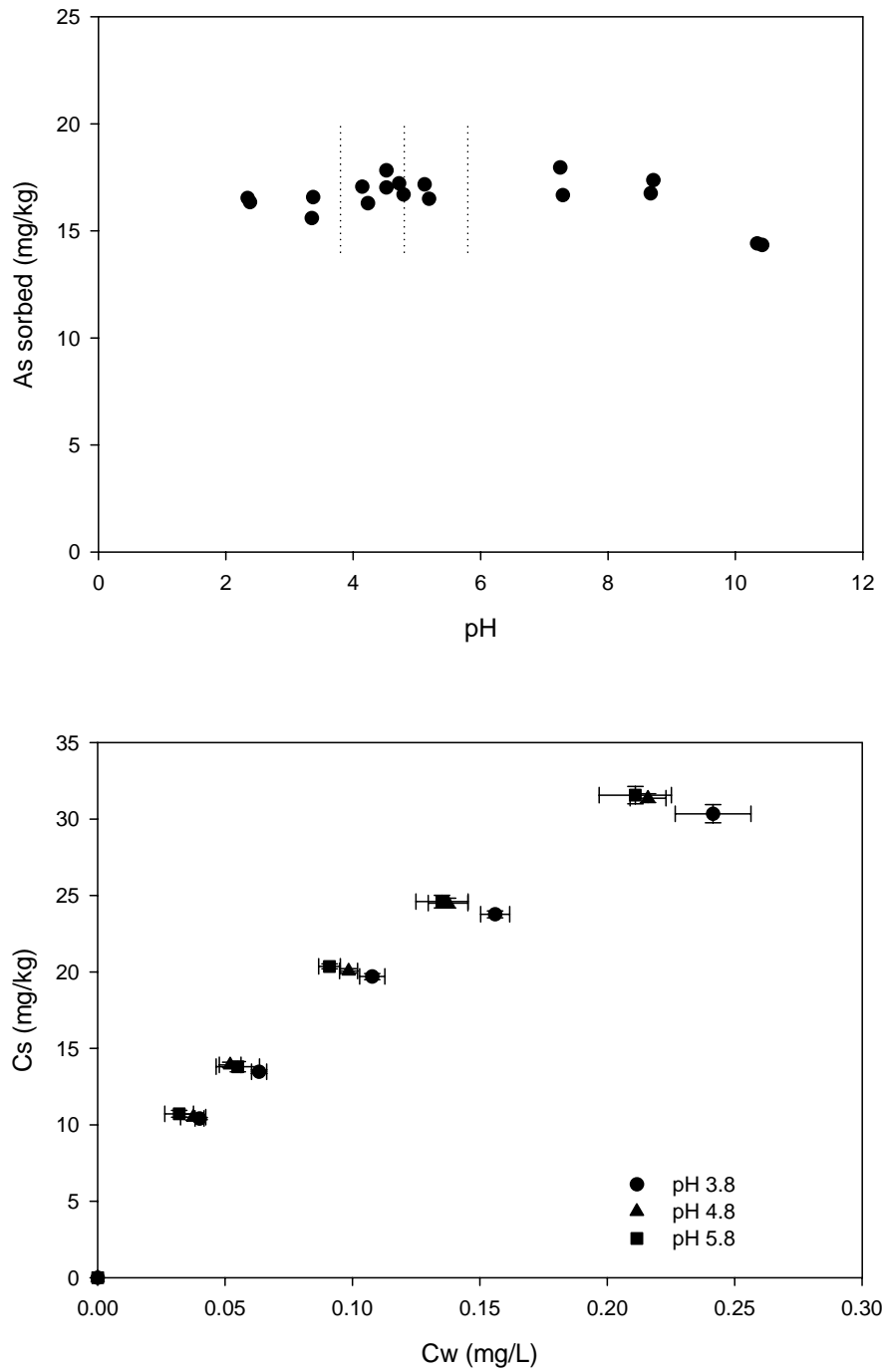


Figure 4-3
pH effects on As(III) adsorption on NE2 10-15: (a) Arsenite adsorption envelope at varying soil suspension pH values; (b) Arsenite adsorption isotherms at pH 3.8, 4.8, and 5.8.

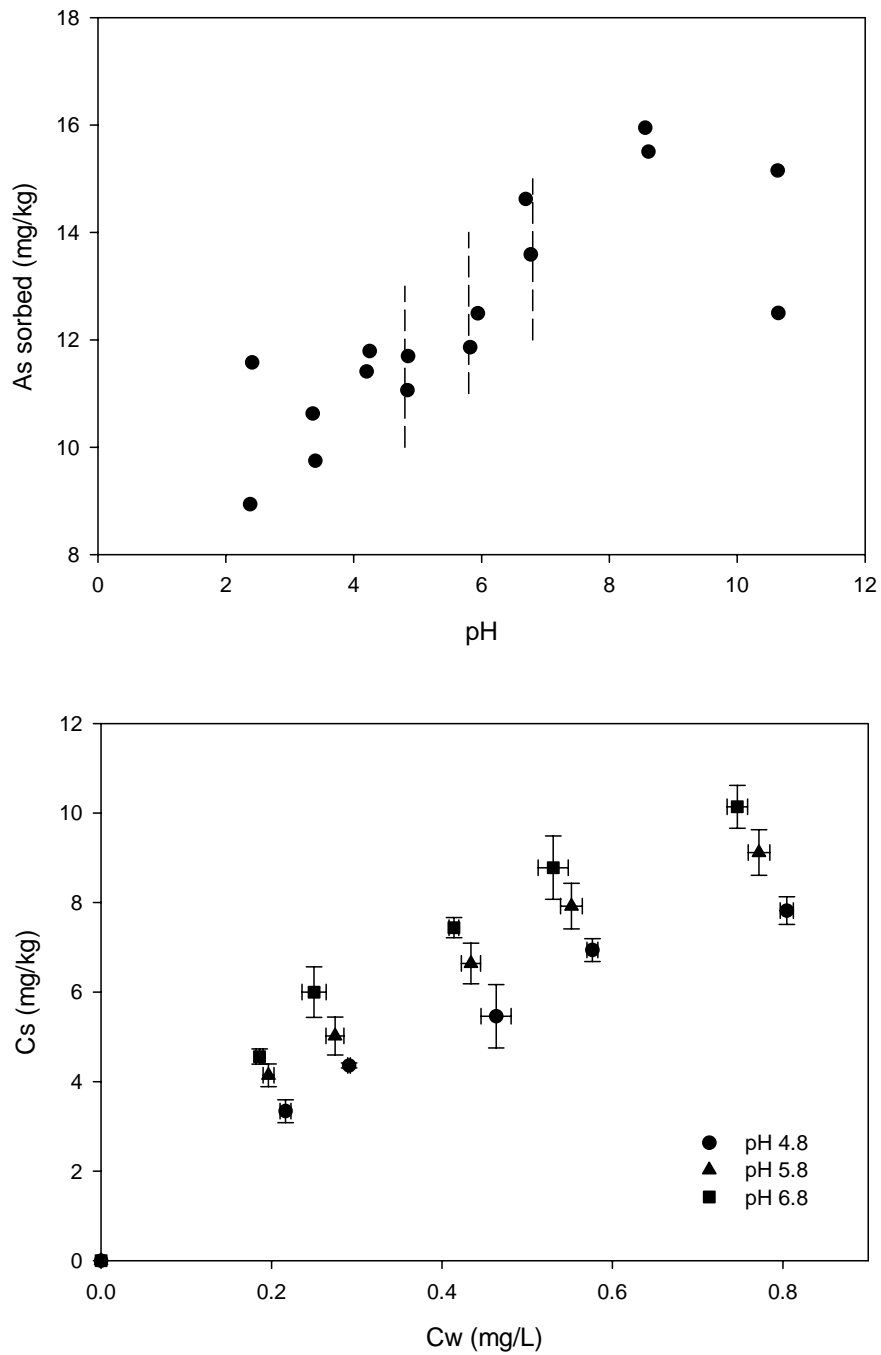


Figure 4-4
 pH effects on As(III) adsorption on NE1 25-30: (a) Arsenite adsorption envelope at varying soil suspension pH values; (b) Arsenite adsorption isotherms at pH 4.8, 5.8, and 6.8.

Solution Matrix Effects on Arsenic Adsorption

The effect of sulfate and calcium on sorption of As(V) and As(III) on two NE site soils is depicted in Figures 4-5 through 4-8, with the upper graph (a) in each figure summarizing the effect of varied sulfate and calcium concentrations on arsenic absorption/adsorption from a fixed concentration of As (1 mg/L for As(V) and 0.75 mg/L for As(III)). The lower graph in each figure is the multi-concentration isotherms from 10^{-3} M KCl ($I = 0.001$ M), 10^{-3} M CaCl₂ ($I = 0.003$ M), 10^{-3} M K₂SO₄ ($I = 0.003$ M), and 10^{-3} M CaSO₄ ($I = 0.004$ M).

Impact of sulfate concentration on adsorption was soil dependent and was most pronounced for As(III). For As(V) at a $C_i = 1$ mg/L, sorption decreased slightly ($C_s = 108$ to 105.2 mg/kg) with increasing sulfate concentrations from 0 to 10^{-2} M on soil sample NE2 10-15 (Figure 4-5a). The decrease was greater (52 to 39.5 mg/kg) on the NE1 25-30 soil (Figure 4-6a), which corresponds to decreases in As(V) sorption of 2.6% and 24%, respectively, for the two site soils. In Figures 4-5b and 4-6b, the single point data collected at the highest sulfate concentration is shown along with the multi-concentration isotherms. Note that the effect of sulfate on As(V) sorption appears to be greater at higher As(V) concentrations. This is most likely due to the fact that As(V) is preferentially sorbed over sulfate on the higher energy sites, but as only the lower energy sites remain (approaching an apparent plateau in isotherm, $N < 1$ phenomenon), sulfate may compete more successfully for sorption sites. For As(III) at a $C_i = 0.75$ mg/L, increasing SO₄ concentrations from 0 to 10^{-2} M resulted in absorbed concentrations decreasing from 24.1 to 15.2 mg/kg for soil sample NE2 10-15 (Figure 4-7a) and from 10.1 to 5.6 mg/kg on soil sample NE1 25-30 (Figure 4-8a), corresponding to decreases in As(III) sorption of 37% and 45%, respectively.

Adsorption of As(V) was enhanced slightly in the presence of increasing concentrations of Ca (Figures 4-5 and 4-6), with the differences between the two soils being similar to what was observed with sulfate, whereas As(III) sorption was not influenced by changes in calcium concentrations (Figure 4-7 and 4-8). As the concentration of Ca was increased from 0 to 10^{-2} M the sorption of As(V) increased from 108 to 109.4 mg/kg on soil sample NE2 10-15 (Figure 4-5a) and 52 to 60 mg kg⁻¹ on soil sample NE1 25-30 (Figure 4-6a), corresponding to increases in As(V) sorption of 1.3% and 15%, respectively. Similar increases in As(V) sorption in the presence of Ca have been reported in soils (Smith et al., 2002); however, little information is currently available concerning the specific mechanism of this enhanced sorption. Plausible explanations for this phenomenon include: (1) sorption of Ca²⁺ to negatively charged surface sites making the electrical potential at those sites less negative, thereby increasing the sorption of arsenate anions; and (2) the formation of intra-molecular bridges between arsenate ions and negatively charged surface sites (e.g., organic matter and alumino-silicate surfaces) by Ca²⁺ ions.

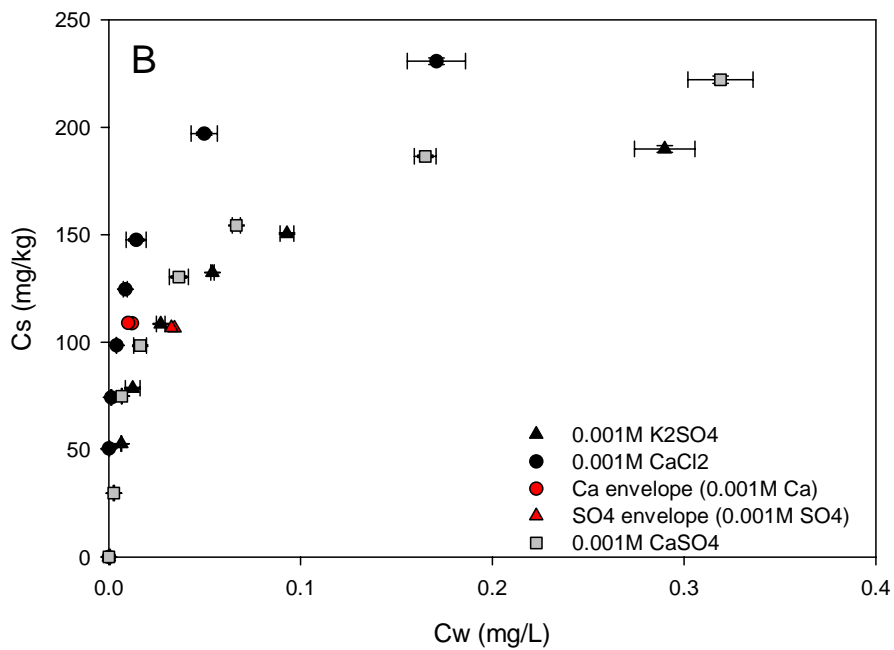
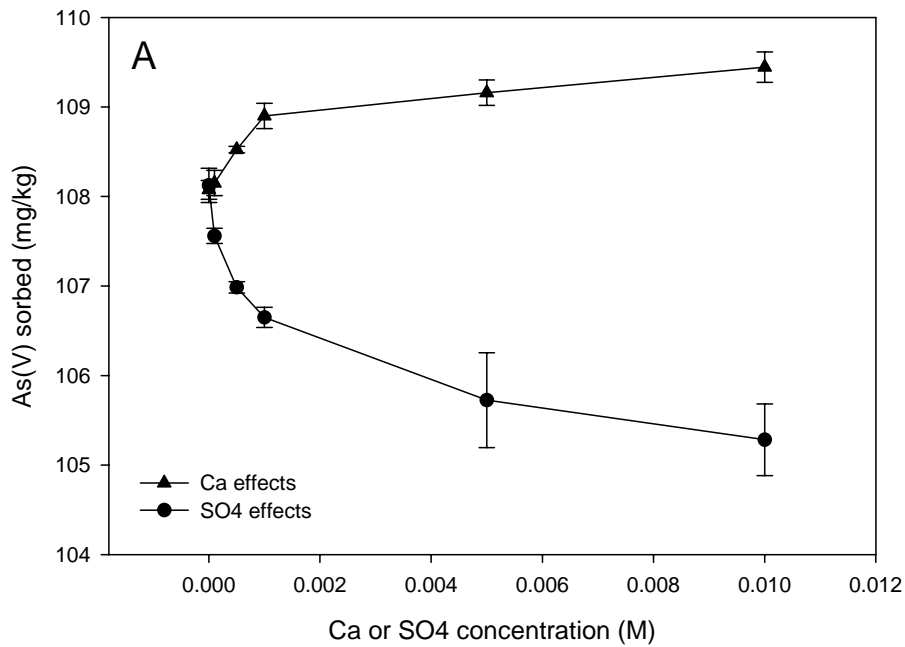


Figure 4-5
 Ionic matrix effects on As(V) sorption onto NE2 10-15: (a) Arsenate adsorption envelopes in the presence of varying concentrations of Ca or SO₄ at a constant ionic strength of 0.03M; (b) Arsenate adsorption isotherms in 0.001M CaCl₂, 0.001M K₂SO₄, and 0.001M CaSO₄.

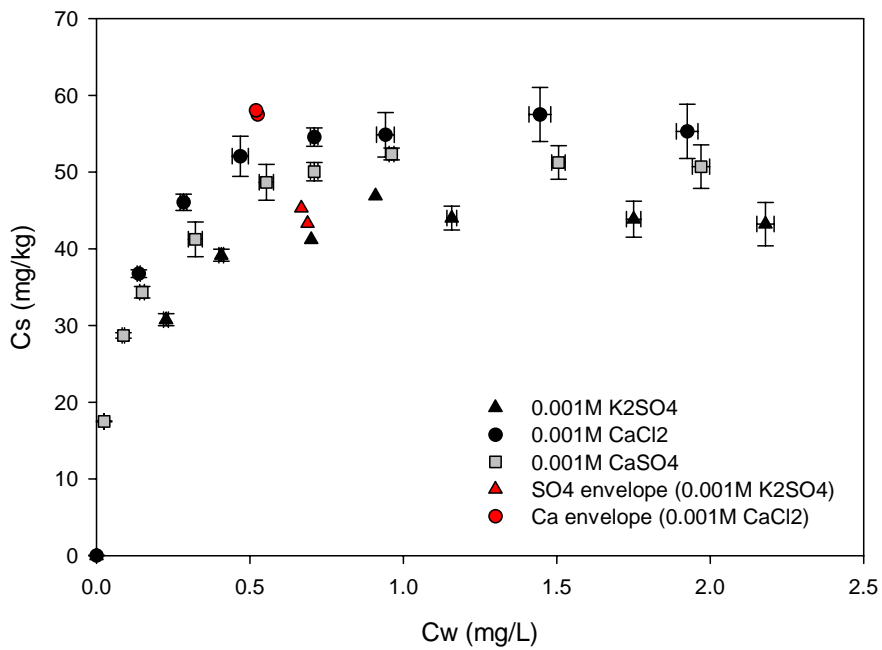
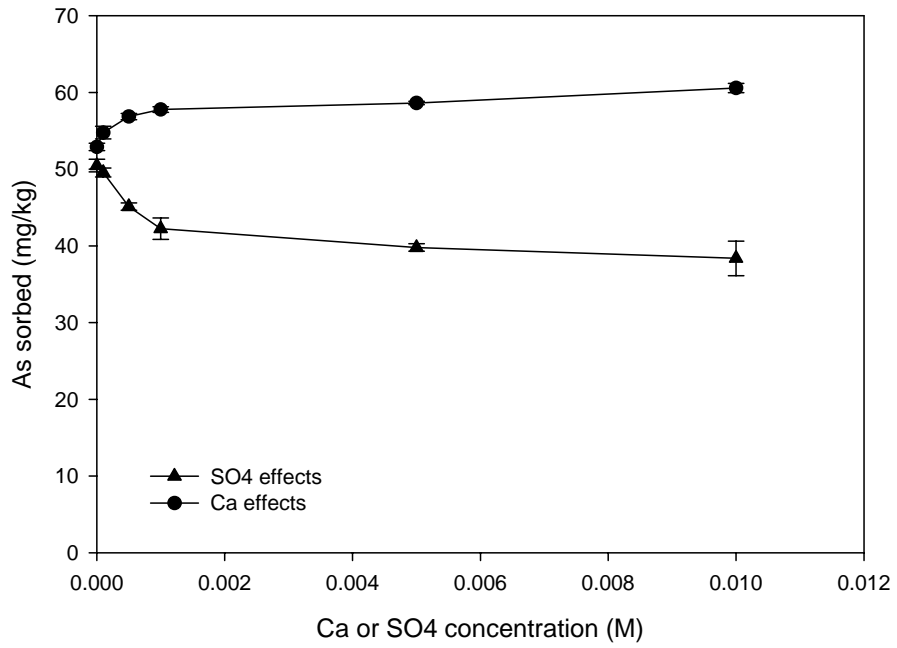


Figure 4-6
 Ionic matrix effects on As(V) sorption onto NE1 25-30: (a) Arsenate adsorption envelopes in the presence of varying concentrations of Ca or SO₄ at a constant ionic strength of 0.03 M; (b) Arsenate adsorption isotherms in 0.001 M CaCl₂, 0.001 M K₂SO₄, and 0.001 M CaSO₄.

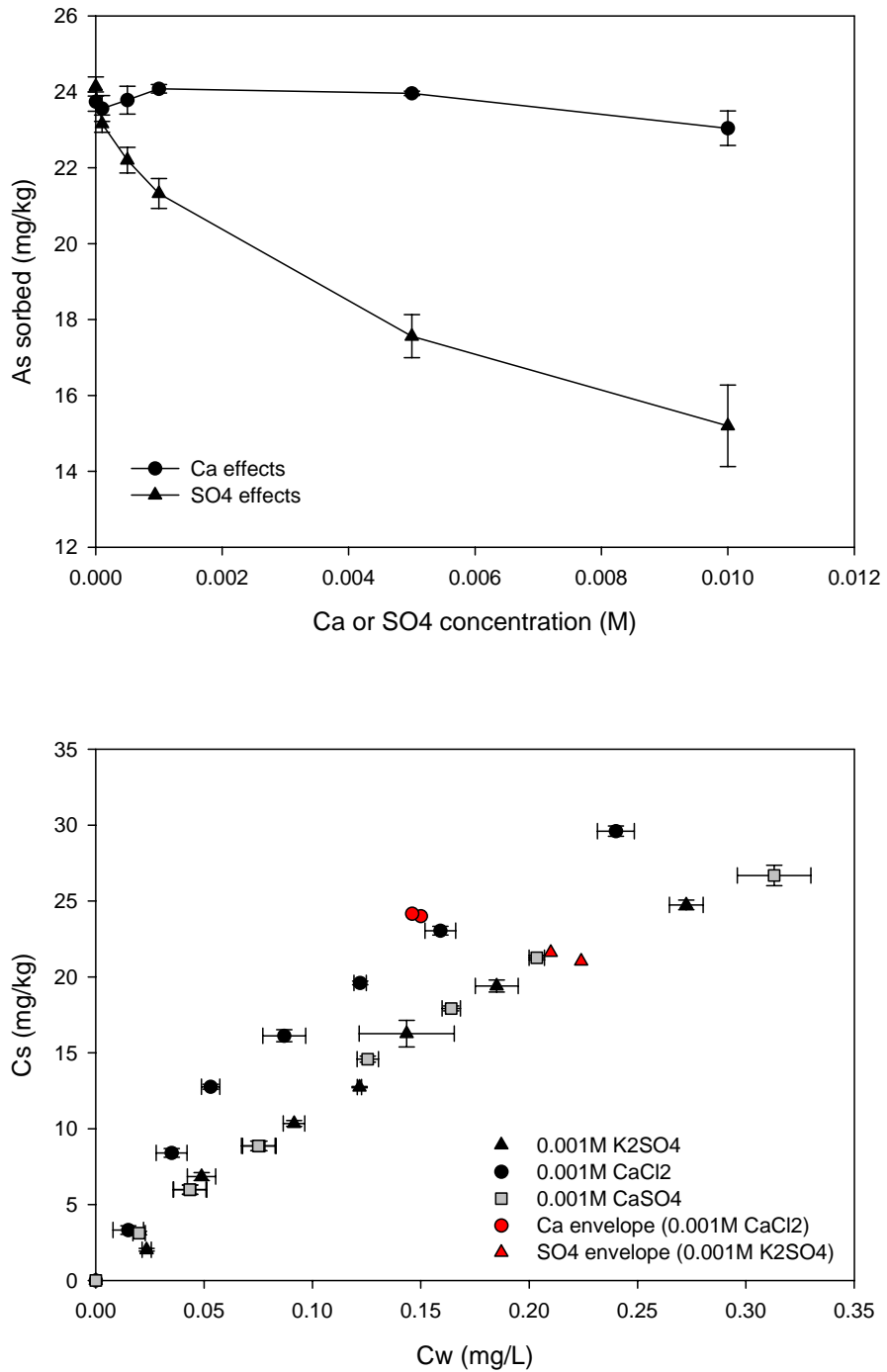


Figure 4-7
Ionic matrix effects on As(III) sorption onto NE2 10-15: (a) Arsenite adsorption envelopes in the presence of varying concentrations of Ca or SO₄ at a constant ionic strength of 0.03 M; (b) Arsenite adsorption isotherms in 0.001 M CaCl₂, 0.001 M K₂SO₄, and 0.001 M CaSO₄.

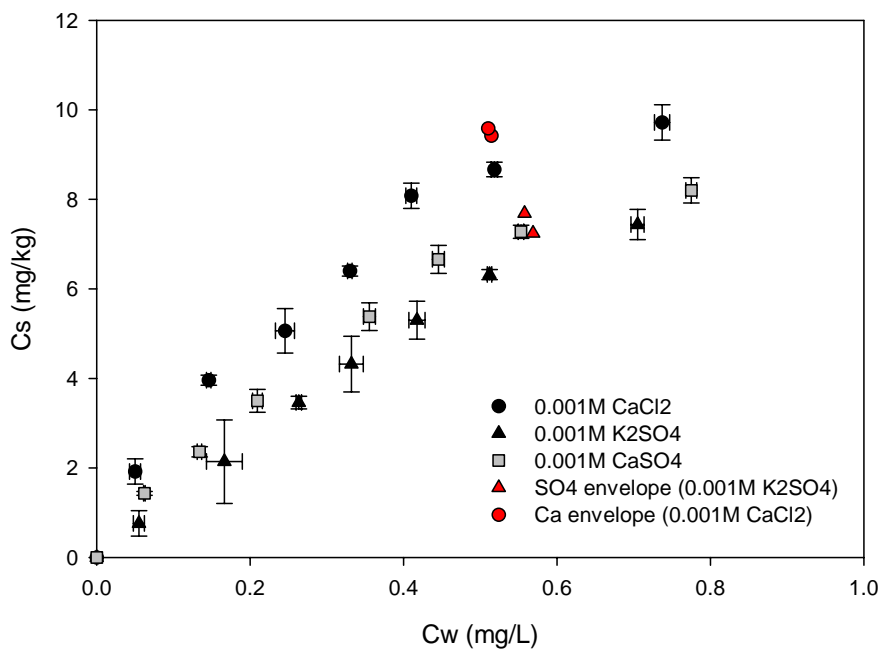
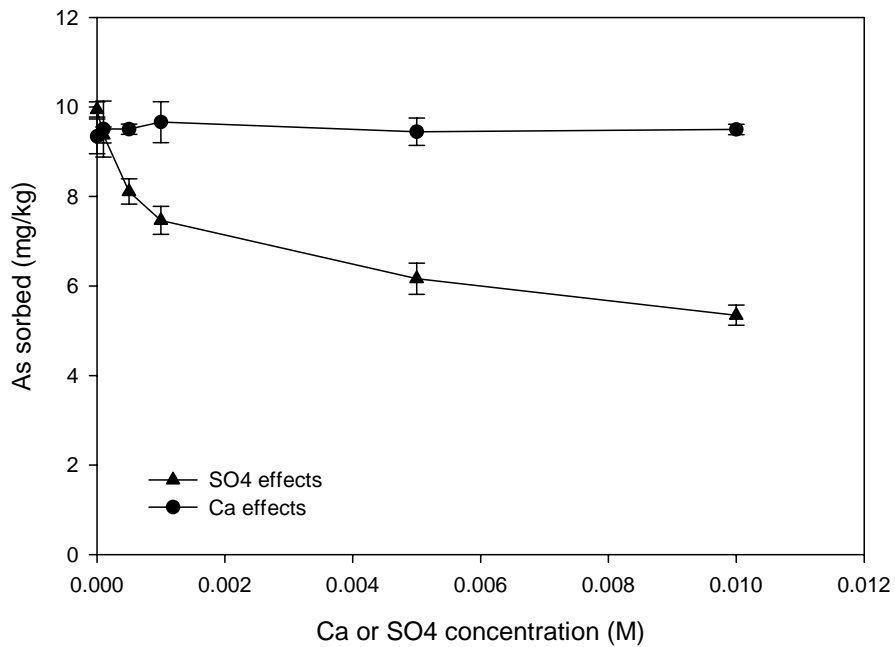


Figure 4-8
Ionic matrix effects on As(III) sorption onto NE1 25-30: (a) Arsenite adsorption envelopes in the presence of varying concentrations of Ca or SO₄ at a constant ionic strength of 0.03 M; (b) Arsenite adsorption isotherms in 0.001 M CaCl₂, 0.001 M K₂SO₄, and 0.001 M CaSO₄.

Sorption Data versus Soil Characteristics for All Sites

Based on previous studies, which have stressed the importance of Fe oxides in establishing adsorption capacities for As in soils (Manning and Goldberg 1997; Elkhatib et al., 1984), it was hypothesized that the Fe oxide content of the soils would be correlated to the adsorptive behavior of As. Linear regression analyses of both the Freundlich K_f and Langmuir model parameters with various soil parameters are summarized in Tables 4-1 and 4-2, respectively. The best correlations observed are with the 15-second DC extractable Fe and either Freundlich K_f values (0.726 and 0.730 for As(V) and As(III), respectively) or the Langmuir $C_{s,max}$ values (0.799 and 0.754 for As(V) and As(III), respectively), clearly exemplifying the role of easily reducible Fe sites in the adsorption of arsenic (Figure 4-9). Reasonable correlations also exist with DC extractable Fe and Al as well as % clay for As(V), and with DC extractable Al and clay for As(III), reflecting oxides in general, which reside in the clay size fraction. No reasonable correlations were obtained with the Langmuir K_L values (Table 4-3).

Table 4-1
Summary of linear regressions between various soil parameters and the mass-based Freundlich isotherm sorption coefficients.

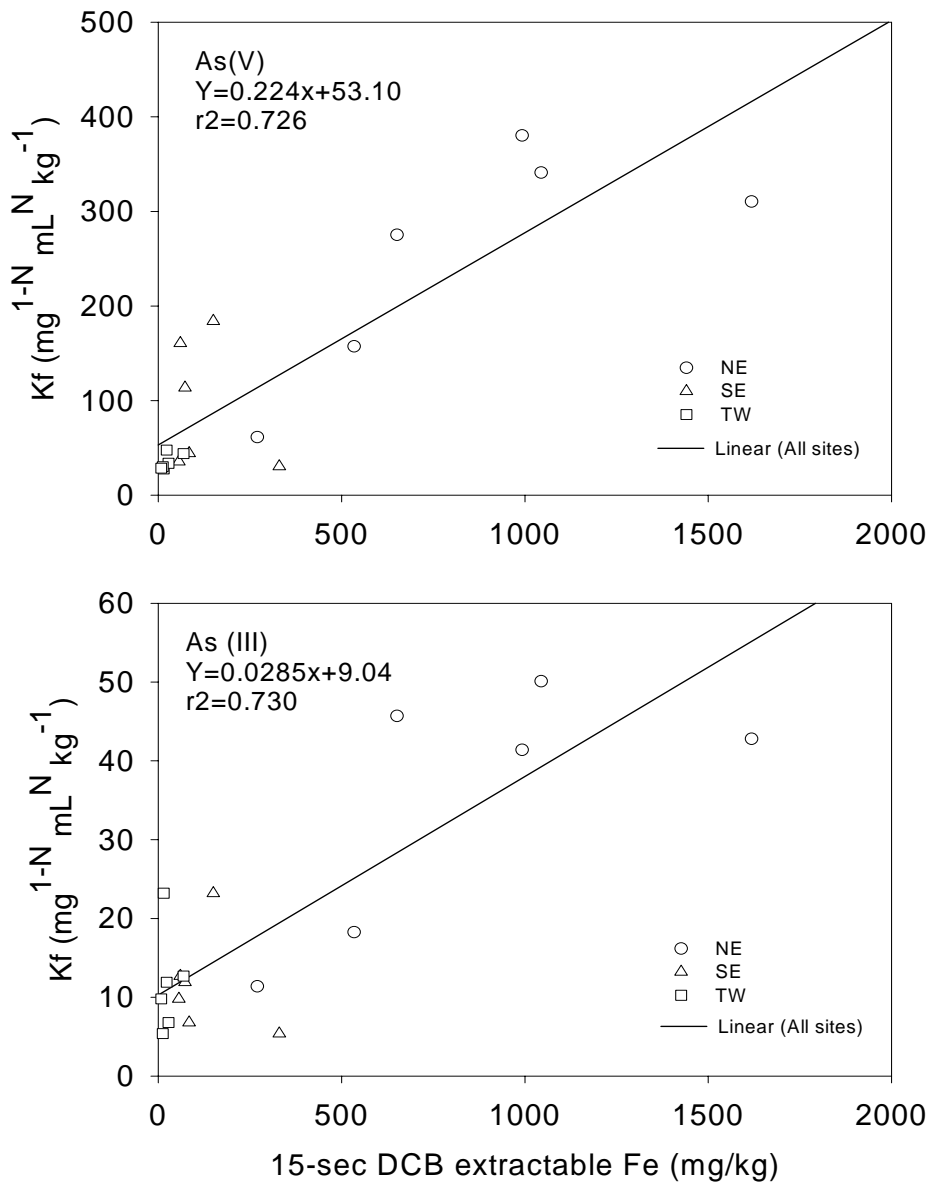
Specie	Regression Parameter	pH _{H2O}	pH _{CaCl2}	% Clay	DC - Fe (mg/kg)	DC - Al (mg/kg)	Ox - Fe (mg/kg)	Ox - Al (mg/kg)	15-sec DCB-Fe (mg/kg)
As(III)	slope	-8.37	-11.27	1.446	0.001	0.031	0.009	0.068	0.029
	intercept	70.93	84.10	6.69	6.51	2.84	10.47	-3.63	9.02
	R2	0.368	0.375	0.658	0.453	0.552	0.533	0.381	0.730
As(V)	slope	-77.52	-107.2	10.85	0.01	0.24	0.06	0.53	0.22
	intercept	611.43	749.99	37.67	19.44	4.18	73.36	-47.30	53.10
	R2	0.528	0.568	0.619	0.599	0.561	0.391	0.391	0.726

Table 4-2
Summary of linear regressions between various soil parameters and the Langmuir model fits for $C_{s, \max}$ (mg/kg).

Specie	Regression Parameter	pH _{H2O}	pH _{CaCl2}	% Clay	DC ⁻ - Fe (mg/kg)	DC ⁻ - Al (mg/kg)	Ox ⁻ - Fe (mg/kg)	Ox ⁻ - Al (mg/kg)	15-sec DCB-Fe (mg/kg)
As(III)	Slope	-4.965	-6.740	0.800	0.001	0.016	0.004	0.032	0.015
	Intercept	45.43	53.58	7.81	7.60	6.58	10.71	3.89	9.30
	R2	0.473	0.490	0.734	0.523	0.497	0.404	0.311	0.754
As(V)	Slope	-73.72	-98.18	10.56	0.01	0.19	0.05	0.44	0.21
	Intercept	577.70	687.57	30.04	29.00	19.94	72.32	-27.47	48.23
	R2	0.606	0.604	0.744	0.510	0.446	0.346	0.342	0.799

Table 4-3
Summary of linear regressions between various soil parameters and the Langmuir model fits for mass-based Langmuir K_L values.

Specie	Regression Parameter	pH* _{H2O}	pH* _{CaCl2}	% Clay	DC ⁻ - Fe (mg/kg)	DC ⁻ - Al (mg/kg)	Ox ⁺ - Fe (mg/kg)	Ox ⁺ - Al (mg/kg)	15-sec DCB-Fe (mg/kg)
As(III)	slope	-3.819	-4.401	0.361	0.0002	0.005	0.004	0.023	0.006
	intercept	33.39	35.11	6.57	7.95	7.00	6.12	1.85	7.67
	R2	0.312	0.233	0.166	0.033	0.059	0.379	0.185	0.114
As(V)	slope	-1.957	-3.516	0.038	0.000	0.008	0.004	-0.047	0.007
	intercept	44.07	52.26	31.55	29.76	28.06	28.02	47.28	29.58
	R2	0.0040	0.0073	0.0001	0.0027	0.0063	0.0228	0.0359	0.0080



5

ATTENUATION OF ARSENIC IN ASH LEACHATE

Leaching and chemical adsorption experiments were performed using leachate generated from site ash samples and soil soils to evaluate the effect of the leachate matrix on arsenic adsorption. Two ash samples from each site were used in sequential and kinetic leaching studies. Ash samples were selected based on their location with respect to the water table. For each site, one ash was selected that resided predominantly above the water table (unsaturated) and one ash was selected that resided predominantly below the water table (saturated). In the case of the SE and MW sites, arsenic was below 10 ppb in the first few leachates of the sequential extractions and was verified to remain as such in a later sequential leaching; therefore, a detailed analysis of the sequential leaching of arsenic was not performed on those ashes. Only arsenic leaching and chemical attenuation data for the ash samples obtained from the NE site are presented in this report.

Sequential Leaching

Average pH values measured for sequential leachings of two NE site ash samples obtained from a depth of 15-20 ft bgs are summarized in Figure 5-1. Arsenic concentrations over the sequential leaching series are shown on Figure 5-2. For both ash samples, the pH increased by about 1 pH unit after the first few sequential leachings and then stabilized at about pH 6.4 to 6.6. As(V) concentrations increased more or less continuously to reach a plateau of about 65 – 80 ppb. As(III) concentrations started low and remained less than 10 ppb for the first 10 leachings before beginning to increase, but remained below 20 ppb for all 15 sequential leachings.

Leaching Kinetics

As(III) and As(V) leaching profiles over time for both NE ash samples are shown in Figure 5-3. In the leaching kinetic study, both As(III) and As(V) increased in concentration over the entire 30-day period. This gradual approach to equilibrium of As dissolution/desorption from ash, which is likely ash dependent, has two practical implications. First, often times laboratory leaching studies result in concentrations that are much lower than those measured in ash leachate wells, which is likely due to be the kinetic process observed in Figure 5-3. The contact time between pore water and the ash (residence time) in the field is usually much longer than the typical 24-h laboratory batch equilibration. Secondly, release concentrations of As from a given ash will not only be dependent on total available arsenic but also on the pore-water velocity at a given site. Therefore, if water travels much slower at one site versus another site, arsenic concentrations in the leachate wells are likely to be higher at that site as well. This kinetic process may also be why arsenic concentrations increase with sequential leaching number, because although the solution phase is being replaced with each leaching, the total time for

which the ash has been water-saturated increases with each leaching step. Therefore, this apparent mass-transfer limited process is also likely to include ash hydration kinetics (kinetics of the wetting process). Changes in pH over time in the kinetic studies were also similar to the sequential leaching studies as shown in Figure 5-1.

Leachate Arsenic Attenuation by NE Site Soils

Chemical attenuation by two NE site soil samples of arsenic species in the ash leachate is shown in Figure 5-4, along with the multi-concentration arsenic isotherms measured from 0.001 M CaSO_4 . As(III) and As(V) present in the ash leachate were significantly attenuated by the acidic soils. The arsenic sorption was consistent with the isotherms developed using 0.001 M CaSO_4 , presented in the previous section. Calcium and sulfate are dominant ions in ash leachate and the use of 0.001 M CaSO_4 appears to be a reasonably good simulated leachate matrix for conducting laboratory equilibrium adsorption tests.

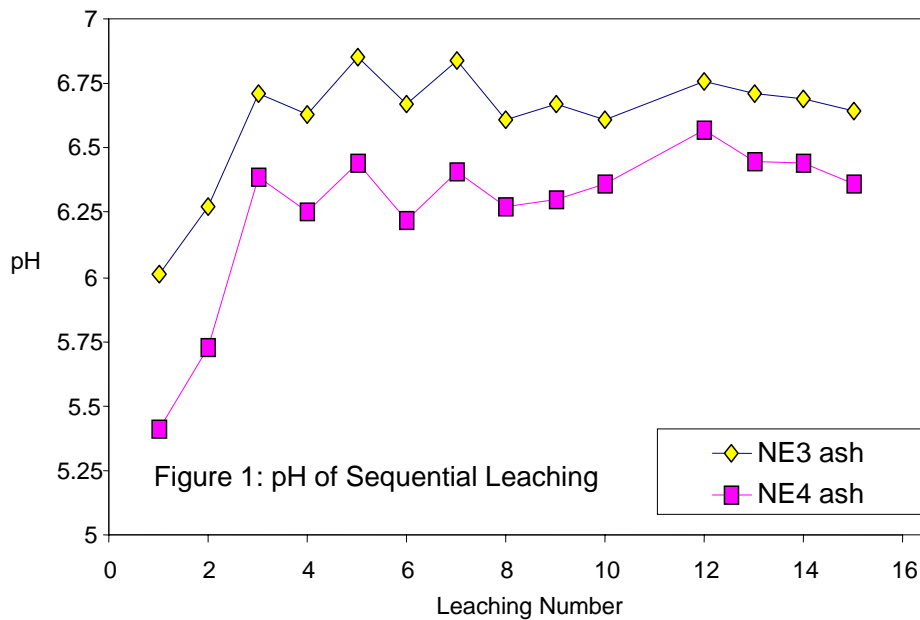


Figure 5-1
pH profile over sequential leaching series for ash samples collected from 15-20 ft depth in two cores at the NE site.

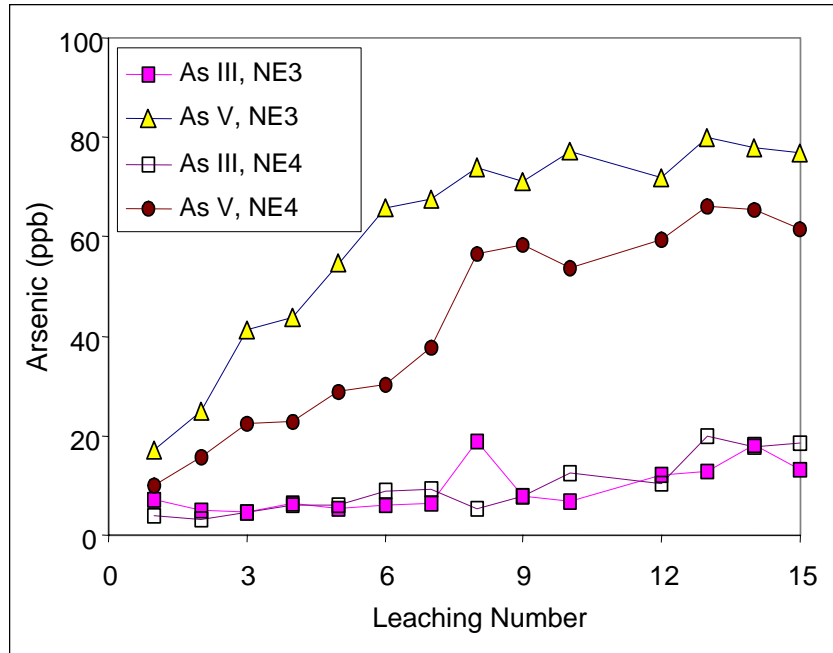


Figure 5-2
As(III) and As(V) profiles over sequential leaching series for ash samples collected from 15-20 ft depth in two cores at the NE site.

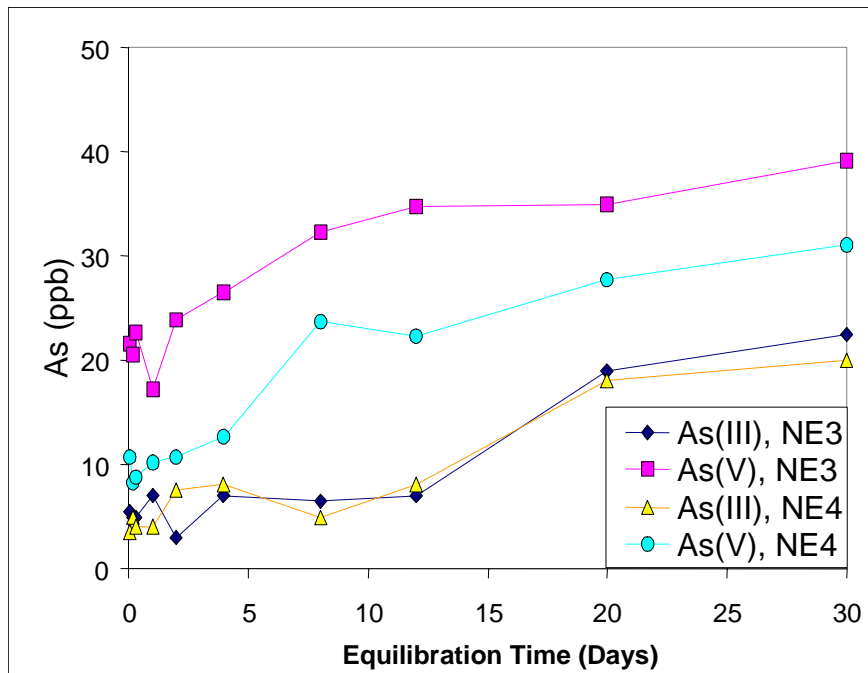


Figure 5-3
Batch leaching of As(III) and As(V) from NE ash samples versus time up to a maximum 30-day equilibration period.

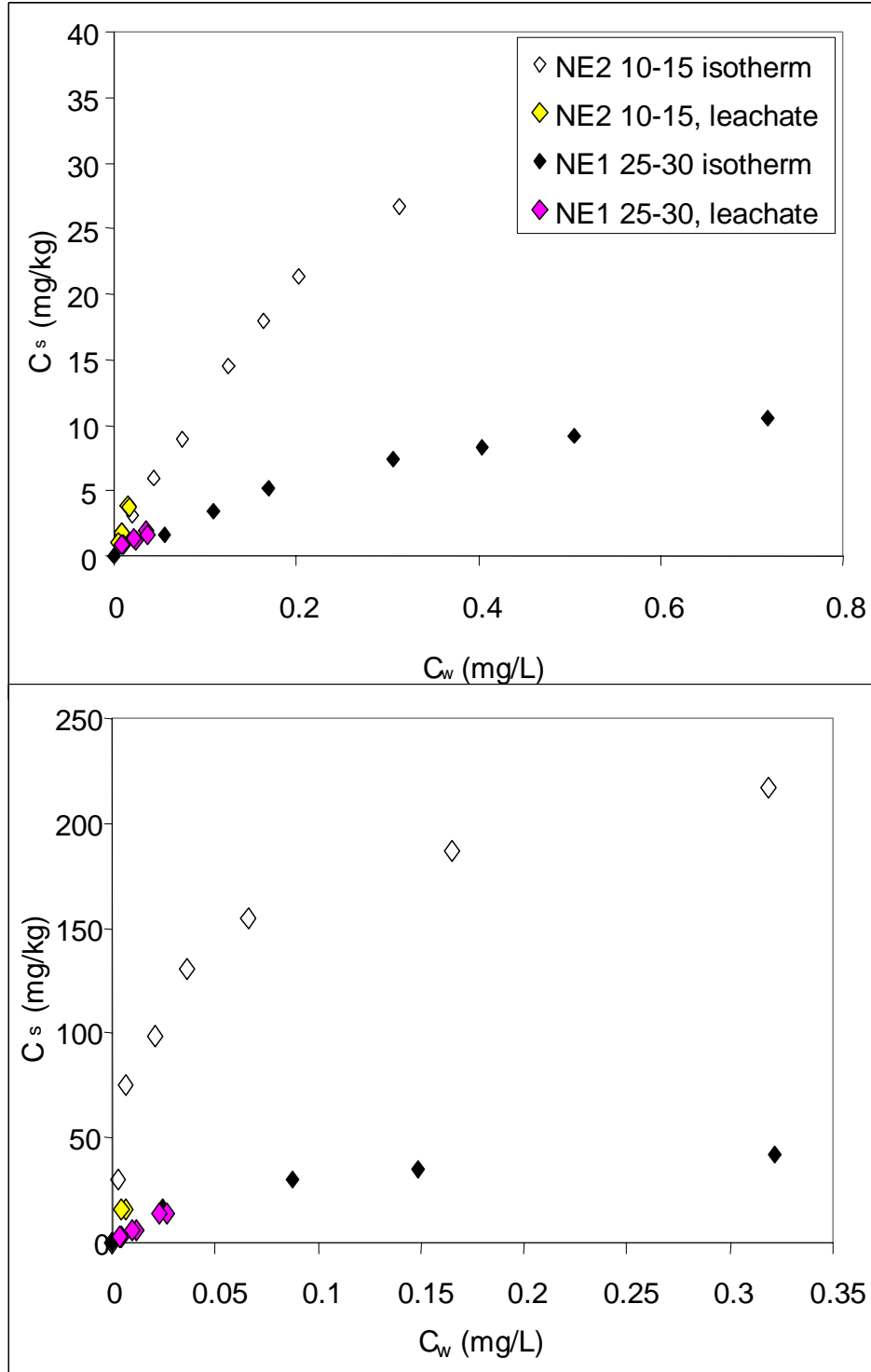


Figure 5-4
Attenuation of As(III) (upper plot) and As(V) (lower plot) present in ash leachate by two NE site soils, and multi-concentration arsenic isotherms measured from 0.001 M CaSO_4 .

6

REFERENCES

- Anderson, M.A., Furguson, J.F., and J. Gavis. 1976. Arsenate adsorption on amorphous aluminum hydroxide. *J. Colloid Interface Sci.* 54:391-399.
- Bolan, N.S., Syers, J.K., and M.E. Sumner. 1993. Calcium-induced sulfate adsorption by soils. *Soil Sci. Soc. Am. J.* 57:691-696.
- Bowden, J.W., Bolland, M.D.A., Posner, A.D., and J.P. Quirk. 1973. Generalised model for anion and cation adsorption at oxide surfaces. *Nature* 245:81-83.
- Bowden, J.W., Posner, A.D., and J.P. Quirk. 1977. Ionic adsorption on variable charge mineral surfaces. Theoretical-charge development and titration curves. *Aust. J. Soil Res.* 15:121-136.
- Brannon, J.M., and W.H. Patrick, Jr. 1987. Fixation, transformation, and mobilization of arsenic in sediments. *Environ. Sci. Technol.* 21:450-459.
- Eary, L.E., Rai, D., Mattigod, S.V., and C.C. Ainsworth. 1990. Geochemical Factors Controlling the Mobilization of Inorganic Constituents from Fossil Fuel Combustion Residues: II Review of the Minor Elements. *J. Environ. Qual.* 19:202-214.
- EPRI, 1987. Chemical Characterization of Fossil Fuel Wastes. EPRI, Palo Alto, CA, Report EA-5321.
- EPRI, 2000. Environmental chemistry of arsenic: a literature review. EPRI, Palo Alto, CA, Report 1000585.
- Goldberg, S., and R.A. Glaubig. 1988. Anion sorption on a calcareous, montmorillonitic soil – arsenic. *Soil Sci. Soc. Am. J.* 52:1297-1300.
- Goldberg, S. 2002. Competitive adsorption of arsenate and arsenite on oxides and clay minerals. *Soil Sci. Soc. Am. J.*, 66:413-421.
- Goldberg, S., and C.T. Johnston. 2001. Mechanisms of arsenic adsorption on amorphous oxides evaluated using macroscopic measurements, Vibrational Spectroscopy, and Surface Complexation Modeling. *J. Colloid Interface Sci.*, 234:204-216
- Gupta, S.K., and K.Y. Chen. 1978. Arsenic removal by adsorption. *J. Water Pollution Control Fed.* 50:493-506.

References

Jackson, B.P., and W.P. Miller. 1998. Arsenic and selenium speciation in coal fly ash extracts by ion chromatography-inductively coupled plasma mass spectrometry. *J. Anal. At. Spectrom.* 13:1107-1112.

Jain, A. and R.H. Loeppert. 2000. Effect of competing anions on the adsorption of arsenate and arsenite by ferrihydrite. *J. Environ. Qual.* 29:1422-1430.

Manning, B.A., and S. Goldberg. 1996. Modeling competitive adsorption of arsenate with phosphate and molybdate on oxide minerals. *Soil Sci. Soc. Am. J.* 60:121-131.

Manning, B.A., and S. Goldberg. 1997. Arsenic(III) and arsenic(V) adsorption on three California soils. *Soil Sci.* 162:886-895.

Manning, B.A., and S. Goldberg. 1996. Modeling arsenate competitive adsorption on kaolinite, montmorillonite and illite. *Clays Clay Miner.* 44:609-623.

Pierce, M.L., and C.B. Moore. 1982. Adsorption of arsenite and arsenate on amorphous iron hydroxide. *Water Res.* 16:1247-1253.

Smith, E., Naidu, R., and A.M. Alston. 2002. Effect of phosphorus, sodium, and calcium on arsenic sorption. *J. Environ. Qual.* 31:557-563.

Theis, T.L. and J.L. Wirth. 1977. Sorptive behavior of trace metals on fly ash in aqueous systems. *Environ. Sci. Technol.* 11:1096-1100.

Theis, T.L., Halvorson, M., Levine, A., Stankunas, A., and D. Unites. 1982. Fly ash attenuation mechanisms. In Report and technical studies on the disposal and utilization of fossil-fuel combustion by-products. Vol. II. Submitted by the Utility Solid Waste Activities Group, the Edison Electric Institute, and the National Rural Electric Cooperative Association to the United States Environmental Protection Agency.

Theis, T.L., and J.L. Wirth. 1977. Sorptive behavior of trace metals on fly ash in aqueous systems. *Environ. Sci. Technol.* 11:1096-1100.

Turner, R.R., 1981. Oxidation state of arsenic in coal ash leachate. *Environ. Sci. Technol.* 15(9):1062-1066.

Wilkie, J.A., and J.G. Ghering. 1996. Adsorption of arsenic onto hydrous ferric oxide. Effects of adsorbate/adsorbent ratios and co-occurring solutes. *Colloids Surf. A: Phys. Chem. Eng. Aspects* 107:97-110.

Xu, H., Allard, B, and A. Grimvail. 1988. Influence of pH and organic substance on the adsorption of As(V) on geological materials. *Water Air Soil Pollut.* 40:293-305.